Human iPSC-derived Microglia Cells Integrated into Mouse Retina and Recapitulated Features of Endogenous Microglia Cells

Wenxin Ma[1], Lian Zhao[2], Biying Xu[3], Robert N. Fariss[4], T. Michael Redmond[5], Jizhong Zou[6], Wai T. Wong[7] and Wei Li[1]

1. Retinal Neurophysiology Section, 2. Genetic Engineering Core, 3. Immunoregulation Section, 4. Biological Imaging Core, 5. Molecular Mechanisms Section, National Eye Institute; 6. iPSC Core, National Heart, Lung, and Blood Institute; 7. Janssen Research and Development LLC, Brisbane, CA, USA.

Correspondence authors: Wai T. Wong: wwong7@its.jnj.com and Wei Li: liwei2@nei.nih.gov

Keywords

Microglia, Retina, hiPSC, Xenotransplantation, Depletion, PLX-5622, Homeostasis, NaIO3, RPE injury

Abstract

Microglia exhibit both maladaptive and adaptive roles in the pathogenesis of neurodegenerative diseases and have emerged as a therapeutic target for central nervous system (CNS) disorders, including those affecting the retina. Replacing maladaptive microglia, such as those impacted by aging or over-activation, with exogenous microglia that enable adaptive functions has been proposed as a potential therapeutic strategy for neurodegenerative diseases. To investigate the potential of microglial cell replacement as a strategy for retinal diseases, we first employed an efficient protocol to generate a significant quantity of human-induced pluripotent stem cells (hiPSC)-derived microglia. These cells demonstrated expression of microglia-enriched genes and showed typical microglial functions such as a robust response to LPS and phagocytosis. We then evaluated the xenotransplantation of these hiPSC-derived microglia into the subretinal space of adult mice that have been pharmacologically depleted of endogenous retinal microglia. Long-term post-transplantation analysis demonstrated that transplanted hiPSC-derived microglia successfully integrated into the mouse retina as ramified cells, occupying the retinal loci previously filled by the endogenous microglia and expresse microglia homeostatic markers such as P2ry12 and Tmem119. Further, these integrated human microglia were found juxtaposed alongside endogenous murine microglia for up to eight months in the retina, indicating their ability to establish a stable homeostatic state in vivo. Following retinal pigment epithelial (RPE) cell injury, transplanted microglia demonstrated responses typical of endogenous microglia, including migration, proliferation, and phagocytosis. Our findings indicate the feasibility of microglial transplantation and integration in the retina and suggest that modulating microglia through depletion and replacement may be a therapeutic strategy for treating neurodegenerative retinal diseases.

Introduction

Microglia are the innate immune cells of the central nervous system (CNS), including the retina, and play pivotal roles in neuronal (Puñal et al., 2019; Anderson et al., 2019; Huang et al., 2012) and vascular development (Checchin et al., 2006; Ritter et al., 2006; Kubota et al., 2009), normal synapse formation (Stevens et al., 2007; Schafer et al., 2012; Schafer et al., 2015; Hong et al., 2016), and maintaining local environmental homeostasis (Li et al., 2018; Colonna et al., 2017; Sierra et al., 2013) and immune activity (Okunuki et al., 2019). Conversely, they are also implicated in driving pathologic progression in various retinal diseases, including age-related macular degeneration (AMD) (Combadière et al., 2007; Ma et al.,

2009, 2012; Karlstetter et al., 2015), glaucoma (Bosco et al., 2019; Ramírez et al., 2020), diabetic retinopathy (Altmann C et al., 2018; Xu et al., 2017), and uveitis (Broderick et al. 2002; Okunuki et al., 2019; Zhou et al., 2020).

Under homeostatic condition in the adult retina, microglia cells are predominantly distributed in the IPL and OPL and vigilantly survey environmental changes through dynamic surveying behavior in their ramified processes (Lee et al., 2008). Their presence and homeostatic function are crucial for maintaining normal retinal functions, including synaptic function and integrity (Wang et al., 2016). Under normal conditions, microglia cells sustain this equilibrium via slow self-renewal (Réu et al., 2017). However, when pathological conditions occur, this homeostasis can be disrupted due to the activation, migration, and proliferation of the cells. Microglia cell repopulation is achieved through the proliferation of endogenous retinal microglia cells and the infiltration of peripheral monocytes (Ma et al., 2017; Huang et al., 2018; Zhang et al., 2018).

Microglia cell repopulation research suggests that: 1) if no injury or infection occurs, retinal microglia cells can sustain their homeostasis indefinitely; 2) following any retinal injury or infection exceeding a certain threshold, the homeostasis of retinal microglia will incorporate macrophages differentiated from peripheral monocytes; and 3) microglia cell replacement could serve as a potential therapeutic approach for retinal diseases. The inhibition of retinal microglia over-activation has proven beneficial for treating retinal diseases (Zhao et al., 2011; Cukras et al., 2012; Karlstetter et al., 2015; Au et al., 2022). In the future, replacing harmful microglia cells with modified, beneficial ones could emerge as a promising therapeutic strategy.

Our understanding of microglia cells stems predominantly from rodent studies, largely due to the accessibility of various transgenic disease models and large-scale cultures. However, several studies have indicated genetic and functional differences between murine and human microglia (Dawson et al., 2018; Friedman et al., 2018; Ueda et al., 2016). For instance, the CD33 and CR1 gene loci associated with Alzheimer's disease (AD), as identified in genome-wide association studies (GWAS), lack reliable orthologues in mice (Hasselmann et al., 2020). Additionally, over half of the AD risk genes are enriched in microglia, demonstrating less than 70% homology between humans and mice (Hasselmann et al., 2020). There are also differences in the protein levels of some complement factors and inflammatory cytokines related to neurodegenerative diseases such as AD and Parkinson’s disease between humans and mice (Galatro et al., 2017; Gosselin et al., 2017; Smith & Dragunow, 2014). As a result, microglia from murine models may not accurately represent many human conditions (Burns et al., 2015).

To surmount these species-specific differences, some investigators have attempted to isolate microglia cells from human tissue. However, owing to limitations in sample resources, detailed genetic background information, and rapid transcriptomic changes that microglia cells undergo post-isolation, these studies have faced numerous constraints and progress has been sluggish (Bohlen et al., 2017; Butovsky et al., 2014; Gosselin et al., 2017). Human-induced pluripotent stem cells (iPSCs) offer a wealth of possibilities across various research fields. Consequently, an increasing number of researchers are now utilizing human iPSCs to differentiate microglia cells (Muffat et al., 2016; Pandya et al., 2017; Abud et al., 2017; Douvaras et al., 2017; Haenseler et al., 2017; Takata et al., 2017; Gao et. 2022), which can provide a large quantity of cells with specific genomic background, possible for establishing an in vivo human microglia cell model through xenotransplantation of human iPSC-derived microglia cells into the murine retina or

brain (Abud et al., 2017; Svoboda et al., 2019; Parajuli et al., 2021; Xu et al., 2020; Chadarevian et al., 2023).

In this study, we applied an appropriate protocol for culturing human iPSC-derived microglia cells, based on established methods (Muffat et al., 2016; Pandya et al., 2017; Abud et al., 2017; Douvaras et al., 2017; Haenseler et al., 2017; Takata et al., 2017). We characterized the microglia cell features by examining microglia-enriched gene expression at both RNA and protein levels. We also assessed the inflammatory responses and phagocytic functions of human iPSC-derived microglia cells in vitro. We then established a human iPSC-derived microglia cell model through the xenotransplantation of human iPSC-derived microglia cells into the retina of an adult mouse. The transplanted human iPSC-derived microglia cells migrated into the retina where native retinal microglia cells reside, with a morphology resembled local mouse microglia cells and expressed microglia signature markers. These grafted cells persisted in the mouse retina for eight months and responded properly to RPE cell injury. These xenografted human iPSC-derived microglia cells can be used to establish a variety of human disease microglia cell models, to serve as a platform for screening therapeutic drugs, and to explore the potential of microglia transplantation as a therapy.

Results

Differentiation and characterization of human iPSC-derived microglia

We used five distinct human iPSC lines for microglia cell differentiation including the very first iPSC line, KYOUDXR0109B, from ATCC, and four others (NCRM6, MS19-ES-H, ND2-AAVS1-iCAG-tdTomato, and NCRM5-AAVS1-CAG-EGFP) obtained from the National Heart, Lung, and Blood Institute (NHLBI). Our approach to differentiation was informed by our previous work with primary mouse retinal microglia cell culture (Ma et al., 2009) and a variety of established microglia cell differentiation protocols (Muffat et al., 2016; Pandya et al., 2017; Abud et al., 2017; Douvaras et al., 2017; Haenseler et al., 2017; Takata et al., 2017). We opted for the myeloid progenitor/microglia cell floating culture method (Van et al., 2013, Haenseler et al., 2017) for its simplicity, efficiency, and consistency, which enables the generation of a large and uniform population of microglia cells.

The differentiation process involved three key stages: embryoid body formation, myeloid progenitor cell generation, and microglia cell maturation (Fig.1, A-D). Following myeloid differentiation, floating myeloid progenitor cells were harvested and allowed to mature for two weeks on 6-well plates under conditions that promoted microglial differentiation. Immunohistochemical analysis of the resulting cells showed that 98.6% of CD34(+) cells were also immunopositive for IBA1 (fig.1E, F), and 98.5% of cells were immunopositive for P2RY12 (Fig.1E, G). Immunostaining with myeloid cell markers CX3CR1, CD68, and CD11b showed positive expression in 88%, 99.7%, and 94.3% of cells, respectively. This demonstrates the high purity and efficiency of our differentiation procedure (Fig.1. suppl). Most iPSC-derived microglia were spindle-shaped, with some displaying short ramifications (Fig.1E), resembling those observed in primary mouse retinal microglia cultures (Ma et al., 2009). The floating myeloid progenitor cells were harvested repeatedly over three months following culture establishment, providing a steady and consistent supply of microglia cells.

A comparative RNAseq analysis between mature microglia cells and floating myeloid cells revealed a high degree of relative microglia-enriched gene expression in mature microglia cells. This included genes such as Cx3cr1, P2ry12, P2ry13, Aif1, Trem2, Gpr34, CD53, CTSS, C3aR1, and others (Fig.2A-C).

Moreover, these microglia cells exhibited a relatively higher expression of genes associated with inflammation, apoptosis regulation, phagocytosis, lipid metabolism, and immune responses. The floating myeloid cells showed higher expression of hematopoietic/myeloid cell lineage genes (Fig. 2D). Graphical analysis results from Ingenuity Pathway Analysis (IPA) identified IL6, IL1b, and Stat3 as central hub signaling pathways, all critical to the regulation of inflammatory responses in microglia cells conditions (Fig. 2E, Fig. 2 suppl). Thus, our method of obtaining differentiated microglia is a reliable method to generate a large number of homogenous, mature microglia cells.

Human iPSC-derived microglia show inflammation responses and phagocytosis activity

Microglia cells play crucial roles in mediating inflammatory responses to stimuli and in phagocytosing pathogens. To further investigate these functions, we stimulated hiPSC-derived microglia cells with lipopolysaccharide (LPS) and analyzed their responses. Graphic analysis of bulk RNA sequencing revealed that the primary responses to LPS stimulation involved IL6, IL1b, IL1a, TNFa, and IFNG signaling (Fig.3A), indicating the ability of hiPSC-derived microglia to demonstrate classical activation. This was confirmed through expression analysis using QPCR and multiplex profiling, which showed a 50 to 800-fold increase in the expression of IL6, IL1a, IL1b, TNFa, IL8, CXCl10, and CCL2 after 6 hours of LPS stimulation (Fig.3B). Similarly, we observed a significant increase in protein levels of these cytokines in cell lysate and culture medium (Fig.3C, D). These results, combined with the high expression of microglia-enriched genes, suggest that the hiPSC-derived microglia cells maintained a steady homeostatic state and exhibited strong responses to LPS stimulation.

Microglia are local immune cells in the CNS, functioning as phagocytes mainly involved in the clearance of apoptotic or necrotic cells, cell debris (Green et al., 2016), and unfolded proteins. They also remodel neuronal connectivity by engulfing synapses, axonal and myelin debris (Paolicelli et al., 2011), and offer protection against infections by directly phagocytosing bacteria and viruses (Nau et al., 2014). To assess the phagocytic capability of hiPSC-derived microglia cells, we exposed them to three different types of bioparticles: E. coli bacteria, zymosan, and bovine photoreceptor outer segments (POS) (Fig.4A-D). The cells altered their morphology to a rounded shape within an hour of incubation and rapidly internalized the fluorescent-labeled particles (Fig.4. Suppl, Fig. 4A-D). The engulfed bioparticles fused into large aggregates around the nucleus, likely within lysosomal bodies. The microglia cells showed active morphological changes as they phagocytosed the POS (Fig.4D, E), resembling the phenotypes observed by retinal microglia phagocytosing photoreceptors in the context of photoreceptor degenerative pathologies in vivo (Zhao et al., 2015).

Homeostasis formation of human iPSC-derived microglia cells in mouse retina after xenotransplantation

To assess the in vivo functionality and replacement potential of hiPSC-derived microglia cells, we conducted xenotransplantation experiments using Reg2-/-;IL2rg-/-;hCSF1+/+ mice as recipients. This is a widely accepted model for transplantation studies as established in previous studies (Svoboda et al., 2019; Xu et al., 2020; Chadarevian et al.,2023). To accommodate the hiPSC-derived microglia cells, we first created an empty microglia niche in the retina using the CSF1R inhibitor PLX-5622 to pharmacologically eliminate microglia in the host retina, thus providing a receptive space for new microglia cell integration (Zhang et al., 2018). Following endogenous microglia depletion in the retina, 1ul of 5000 hiPSC-derived microglia cells were transplanted into the subretinal space (Fig.5A). Tissue analysis at 4 and 8 months post-transplantation revealed that transplanted cells, which were marked by

tdTomato expression, had migrated from the subretinal space into the neural retina and were distributed across a wide retinal area within inner and outer retinal layers, including the ganglion cell layer (GCL), inner plexiform layer (IPL), and outer plexiform layer (OPL) (Fig.5B-D), in the retinal loci typically occupied by endogenous microglia. Transplanted cells were immunopositive for Iba1, and human CD11b (Fig.5C), as well as microglia signature markers P2ry12 and TMEM119 (Fig.5D). Interestingly, the transplanted cells within the retina showed a ramified morphology and a regularly tiled "mosaic" distribution in their soma positions, and were juxtaposed alongside endogenous murine microglia cells, which showed a similar morphology and distribution, indicating that transplanted hiPSC-derived microglia were responded to similar intraretinal cues to be organized spatially, morphologically, with similar neighbor-neighbor interactions as with the endogenous murine microglia population (Fig.5E-G). Similar observations were also made when the alternate EGFP-expressing hiPSC-derived microglia were transplanted confirming that these results can be generalized to other hiPSC-derived microglia cells (Fig.5H).

We further evaluated the impact of human iPSC-derived microglia cell xenotransplantation on the host mouse retinal cells (Fig. 5 supple A-D). Immunostaining using Glial fibrillary acidic protein (GFAP) and Glutamine Synthetase (GS) antibody (Fig. 5 supple A, B) indicated that the transplanted human iPSC-derived microglia cells did not trigger any gliosis or reactive proliferation in Muller cells four months post-transplantation. Additionally, the morphology and distribution of other retinal cells, including ganglion cells, Muller glia cells, horizontal/amacrine cells, bipolar cells, and cone photoreceptor cells, remained normal (Fig. 5 supple A-D), indicating that microglia transplantation had no adverse impact on the structural integrity of retinal architecture. Furthermore, staining with the mouse CD11b antibody showed that the transplanted human iPSC-derived microglia cells did not displace the native retinal microglia cells even after four months post-transplantation (Fig. 5 supple E, F), indicating the ability of these human iPSC-derived microglia cells to integrate harmoniously with the existing microglial population in the mouse retina.

Grafted homeostatic hiPSC-derived microglia cells respond to RPE cell injury with migration and proliferation

The xenotransplanted human iPSC-derived microglia cells established a new equilibrium with the original mouse retinal microglia cells four months post-transplantation. To monitor the longer-term consequences of transplantation, we extended our analysis to up to 8 months post-transplantation. The retinal flat mount confirmed that the tdTomato+ cells were still appropriately located in the GCL, IPL, and OPL, forming a tile-like distribution typical of microglial homeostasis (Fig.6 Suppl A, B). The transplanted human iPSC-derived microglia cells maintained expression of hP2ry12 and hTMEM119, markers of mature retinal microglia, which suggests that they were well tolerated within the mouse tissue (Fig.6 Suppl A, B).

To further evaluate the function of the transplanted microglia in the mouse retina and their ability to respond to injury in vivo, we subjected recipient mice to sodium iodate (NaIO3)-mediated RPE injury 240 days following transplantation and analyzed retinal tissue 3 and 7 days following injury (Fig 6A). In a previous study (Ma et al., 2015), we had characterized the responses of endogenous microglia in this injury model; in the days following injury, endogenous microglia within the neural retina migrated into the subretinal space to come into close proximity to damaged RPE cells. This resulted in, a transient decrease in microglia number in the IPL and OPL, which then recovered following proliferation of the

remaining microglia to replenish the depleted areas. We found that transplanted hiPSC-derived microglia demonstrated responses similar to endogenous microglia. Three days after NaIO3 injury, there was an increase in tdTomato+ and P2ry12+ human iPSC-derived microglia in the subretinal space, while their number decreased in the IPL and OPL (Fig.6B-D, G). Some of the remaining tdTomato+ and P2ry12+ cells were positive for the cell-proliferation marker Ki67, indicating active cell division (Fig.6B-D, F). Ki67+ tdTomato+ cell numbers peaked at three days post-injury and decreased by day seven (Fig.6B-F). Seven days post-injury, the numbers of tdTomato+ and P2ry12+ human iPSC-derived microglia increased in the IPL and OPL but decreased in the subretinal space (Fig.6E, G); Ki67+ tdTomato+ cell numbers also declined (Fig.6E, F). This suggested that once the cells had filled the empty spaces in the retina, their division ceased. This response mirrors that of the original mouse retinal microglia to NaIO3 injury (Ma et al., 2015).

Overall, these results demonstrate that the transplanted human iPSC-derived microglia cells not only integrate into the neural retina alongside endogenous retinal microglia under baseline conditions but also exhibit a similar migration and proliferative response to injury.

hiPSC-derived microglia cells phagocytize debris or dead photoreceptor cells after NaIO3-induced RPE cell injury

Phagocytosis, a critical function of microglia, plays an essential role during both developmental stages and pathological processes. For instance, retinal microglia phagocytose unhealthy photoreceptors in the rd10 mouse model of photoreceptor degeneration and clear apoptotic photoreceptors (Zhao et al., 2015; Silverman et al., 2019). Following three days of RPE cell injury induced by NaIO3, the tdTomato+ hiPSC-derived transplanted microglia migrate not only to the subretinal space but also into the photoreceptor layer (Fig.7A), coincident with the development of photoreceptor degeneration and disorganization, including the onset of abnormal morphology of arrestin+ cone photoreceptors, and a decrease in photoreceptor density (Fig.7A).

The increase in microglia in the subretinal space and photoreceptor layer (Fig.7A-C) initiates the clearance of dead cells, as evidenced by the accumulation of autofluorescent material in the microglia cell bodies (Fig.7A, B, D). These tdTomato+ microglia cells undergo morphological changes, losing their normal processes and transforming into larger amoeboid cells (Fig. 7B, yellow triangle) that contain arrestin+ photoreceptor debris, indicating the ability of transplanted microglia to enable engulfment of degenerated photoreceptors (Fig.7B). Such observations further demonstrate that the xenografted human iPSC-derived microglia cells perform functions that closely mimic those of normal retinal microglia cells in vivo.

Discussion

Microglia cells are instrumental in the development and progression of numerous CNS diseases. For instance, in Alzheimer's disease, microglia are enriched in over 50% of associated gene loci implicated in AD risk (Hasselmann et al., 2020). Similarly, in Age-related Macular Degeneration, 57% of 368 genes, located close to 52 AMD gene loci, are expressed in retinal microglia cells (Fig. discussion suppl B), and 52% of them are highly expressed in these cells (Fig. discussion suppl A & B; Fritsche et al., 2016; Ma et al., 2013; Den et al., 2022). Understanding microglia cell functions is essential for investigating disease mechanisms and identifying accurate therapeutic targets. Most of our current knowledge about microglia cells comes from rodent studies. However, genetic and functional differences exist between

murine and human microglia (Galatro et al., 2017; Gosselin et al., 2017; Smith & Dragunow, 2014). Hence, more in-depth knowledge of human microglia cells in vitro and in vivo is required.

Human-induced pluripotent stem cells (iPSC) offer promising prospects for many retinal research fields (Zhong et al., 2014; Leach et al.,2016; Tanaka et al., 2016). For over a decade, macrophage/microglia cells have been differentiated using human iPSC (Karlsson et al., 2008; Pocock et al., 2018; Gao et. 2022). An abundance of hiPSC-derived microglia cells, with defined genomic background, and easy manipulation of hiPSC offer substantial benefits in various research areas.

Under in vivo physiological conditions, microglia cells exhibit a tile-like arrangement, without overlap. They try to maintain this property in culture, allowing overgrown cells to float out to the medium. Based on this phenomenon and a variety of established microglia cell differentiation protocols (Muffat et al., 2016; Pandya et al., 2017; Abud et al., 2017; Douvaras et al., 2017; Haenseler et al., 2017; Takata et al., 2017), we opted for the myeloid progenitor/microglia cell floating culture method (Van et al., 2013, Haenseler et al., 2017) for its simplicity, efficiency, and consistency, which enables the generation of a large and uniform population of myeloid progenitor cells (>98.6% CD34+) over three months. These progenitor cells differentiate into pure mature microglia cells (>98.5% P2ry12+), bearing a profile rich in microglia genes, and demonstrate characteristics similar to native microglia in physiological CNS tissue. A comparison of the signaling pathway to myeloid cells reveals the central hubs of signaling as IL6, IL1b, and the stat3 pathway (Fig.2D), which are key to microglia functioning during inflammation. The differentiation protocol employing floating myeloid progenitor cells produces a significant number of CNS resident-like microglia cells. These hiPSC-derived cells respond robustly to LPS stimulation and demonstrate phagocytic activity, mimicking primary cultured retinal microglia cells. Therefore, they effectively replicate resident microglia characteristics (Ulland et al., 2018; Wang et al., 2020; Shi et al., 2022; Guo et al., 2022).

CNS disease treatment strategies include gene regulation, gene delivery (Neumann et al., 2006; Beutner et al., 2013), rejuvenation (Karlstetter et al., 2015; Elmore et al., 2018), or replacement of dysfunctional microglia cells (Willis et al., 2020; Xu et al., 2020; Han et al., 2020; Shibuya et al., 2022). hiPSC-derived microglia cells offer a potentially unlimited source for cell replacement therapy. The in vivo functionality of these cells was verified through xenografting into adult Reg2-/-; IL2rg-/-;hCSF1+/+ mice. The grafted cells integrated well, expressing microglia signature genes and maintaining homeostasis for eight months. They responded to RPE cell injury like host retinal microglia cells, marking the success of the xenotransplantation model (Guilliams et al., 2017) and highlighting the potential for hiPSC-derived microglia cells in retinal microglia cell replacement therapy, such as in AMD.

Several exogenous microglia cell replacement techniques have been investigated, with these methods varying based on the type of donor cells used and the age of the recipient. Initial microglia cell replacement studies involved the transplantation of hematopoietic stem cells (HPSC) (Larochelle et al., 2016; Xu et al., 2020; Hohsfield et al., 2020). However, even after differentiation in local tissue, HPSC-derived microglia cells maintained some gene expressions distinct from the original resident microglia cells (Lund et al., 2018), warranting further exploration of these HPSC-derived microglia cells' unique characteristics. Another method involves the use of newborn mice as recipients, with iPSC or SC-derived microglia cells as the donors (Mancuso et al., 2019; Xu et al., 2020). This approach does not require the depletion of resident microglia cells, and the grafted cells can infiltrate the brain tissue, distributing

similarly to the original resident microglia cells. While suitable for examining microglia cell function in various backgrounds, the clinical applicability of this method remains limited.

A third transplantation approach involves adult recipients receiving iPSC or SC-derived microglia cells after resident microglia cell depletion (Chadarevian et al., 2023). Since this technique requires a microglial-empty niche, resident microglia must be depleted or relocated from the retina, typically done using CSF1R inhibitors. To prevent these inhibitors from affecting the grafted cells, investigators have tried using modified CSF1R microglia cells as donor cells (Chadarevian et al., 2023). In our research, we found a two-day recovery period with normal food intake sufficient to clear the CSF1R inhibitor, allowing grafted cells to integrate into an undisturbed niche. In this study, we used the subretinal xenotransplantation method, though alternative transplantation routes such as intravenous injection, vitreous, and suborbital space delivery warrant further exploration.

In conclusion, hiPSCs can be differentiated into microglia cells through a simplified common pathway and factors, although the precise differentiation factors still need further investigation under in vitro conditions. For instance, the microglia signature gene, TMEM119, shows low expression in hiPSC-derived microglia culture conditions. Interestingly, we discovered that a medium composed of mixed cultured embryoid bodies and microglia progenitor cells fosters further differentiation of microglia cells. The humanized mouse model established through xenotransplantation serves as a reliable tool for studying the functions of various hiPSC-derived microglia cells. This model offers a valuable platform for investigating disease mechanisms and evaluating the therapeutic effects of xenografted hiPSC-derived microglia cells from diverse patient backgrounds.

EXPERIMENTAL PROCEDURES

Experimental animals and PLX-5622 treatment

The immunodeficiency and human CSF1 knockin mice Rag2−/−;Il2rg-/-;hCSF1+/+ was purchased from Jax Lab (#17708). Experiments were conducted according to protocols approved by Institutional Animal Care and Use Committee (National Eye Institute Animal Care and Use Committee) and adhered to the Association for Research in Vision and Ophthalmology. Statement on animal use in ophthalmic and vision research. Animals were housed in a National Institutes of Health (NIH) animal facility under a 12-h light/dark cycle with normal food. The results of sequencing of Crb1 revealed no rd8 mutation in these mice. To produce microglia empty niche, the retinal microglia cells were depleted with the dietary administration containing PLX5622 (Plexxikon), a potent and selective inhibitor of the CSF1R, previously demonstrated to deplete microglia in the brain (Dagher et al., 2015) and retina (Zhang et al., 2018). 2-month-old animals were placed on a rodent chow containing PLX5622 (at 1200 parts per million) for ten days, and then switched back to a normal standard chow; on the third day of normal diet resumption, the cultured hiPSC-derived microglia cells were grafted into the subretinal space.

Human iPSC Culture

The five human iPSC lines were used in this study. The KYOUDXR0109B (201B7, ATCC:ACS1023) hiPSC line was generated in Yamanaka Lab with female health Fibroblasts and reprogrammed by the expression of OCT4, SOX2, KLF4 and MYC using retroviral transduction; NCRM5-AAVS1-CAG-EGFP (clone 5), ND2-AAVS1-iCAG-tdTomato (clone 1), NCRM6 and MS19-ES-H were obtained from or generated by NHLBI iPSC Core Facility of National Heart, Lung and Blood Institute (NHLBI). NCRM5-AAVS1-CAG-EGFP is

EGFP reporter iPSC line with CAG-EGFP targeted mono-allelically at AAVS1 safe harbor in NCRM5 iPSC which was reprogrammed from health male CD34+ PBMC, ND2-AAVS1-iCAG-tdTomato is tdTomato reporter iPSC line with insulated CAG-tdTomato targeted mono-allelically at AAVS1 safe harbor in ND2 iPSC which was reprogrammed using health male fibroblast cells; The microglia cells differentiated from these 2 lines were used for the transplantation. NCRM6 iPSC line was reprogrammed from a healthy female CD34+ PBMC with Episomal vectors; MS19-ES-H line was reprogrammed from a healthy female PBMC with Cytotune Sendai Virus kit.

The derivation and characterization of iPSC lines have been done in ATCC and NHLBI iPSC Core Facility. Cells were maintained on Geltrex (0.2mg/ml, Gibco, #A1413302) coated 6-well plate with 1x mTeSRTM-1 medium and passaged with TrypLE Express (Gibco by Life Technologies) and plated in medium containing 3uM Rho-kinase inhibitor Y-27632 (Abcam) at the first time, change medium 100% every day. 70% of confluence cells were passaged or frozen in Stem Cell Freezing Media (mFreSR™, StemCells, Catalog # 05854).

Myeloid progenitor cells differentiation and microglia cells maturation

The procedure of myeloid cell linage and microglia cell differentiation was based on Sara Cowley's Lab protocol (Van et al., 2013, Haenseler et al., 2017), plus modifications. The microglia cell differentiation through 3 steps: 1) Embryoid Body (EB) formation: using Spin-EBs formation method with AggreWellsTM800 (Stemcell Technologies, Catalog # 34825). briefly, 1 mL of mTeSRTM-1 spin-EB medium was added to the AggreWell and centrifuged at 3000 g for 2 minutes, 1 mL of $4x10^6$ iPSC was added per well, the plate containing iPSC and 2 mL of spin-EB medium per well was centrifuged at 800 rpm for 3 minutes. The plate was incubated in the incubator at 37°C, 5% CO2 for four days, then 1 mL medium was replaced in a drop-wise manner every day. After day 4 (total day 8), the EBs were harvested with a 40um filter column. The EB media: mTeSR1 (STEMCELL Technologies), 50 ng/mL BMP-4 (GIBCO- PHC9534), 20 ng/mL stem cell factor (Miltenyi Biotec), 50 ng/mL vascular endothelial growth factor (GIBCO- PHC9394); 2) Myeloid progenitor cell generation: after EB counting, the 150-200 EBs were transferred to 75-cm^2 flask with myeloid cell differentiation medium: TheraPEAK™ X-VIVO™-15 Serum-free Hematopoietic Cell Medium (Lonza, Cat#: BEBP04-744Q), 100 ng/mL M-CSF (Invitrogen), 25 ng/mL IL-3 (R&D), 2 mM glutamax (Invitrogen), 1xN2 supplement (Thermofisher Scientific, Cat#17502048). Two-thirds of the media was changed every five days. After 2-3 weeks of culture, non-adherent single-layer floating cells were harvested from the supernatant. These cells are myeloid cell lineage-myeloid progenitor cells. 3) Microglia cell maturation: The single layer of floating connected flakes-like cells were harvested with the medium and transferred into the 6-well plate to continue the culture. When the cells adherend to the bottom of the well on the next day, change 2/3 medium with microglia cell differentiation medium: DMEM/F12 (gibco, #11330), 50 ng/mL M-CSF (Invitrogen), 100 ng/mL IL-34 (Peprotech), 10 ng/mL TGFb1(R&D), 2-5ng/ml TGFb2(R&D), 20ng/ml CX3CL1(Peprotech) and N2 supplement, 2 mM Glutamax. If the cell number too low from 1st time harvested, then harvest one more time after the next day into the same 6-well plate to cumulate the cells. The cells were cultured for two weeks and then went to the next step assay or harvest for cell transplantation.

Phagocytosis Assay

To evaluate the phagocytosis capabilities of hiPSC-derived microglia cells, we used 3 challenge bioparticles to attack the receptor TLR4, TLR2, TLT6, and other pathogen receptors. 1) pHrodo™ Red E. coli BioParticles Conjugate for Phagocytosis (ThermoFisher Scientific, cat# P35361); 2) pHrodo™ Red

Zymosan Bioparticles™ Conjugate for Phagocytosis (ThermoFisher Scientific, cat# P35364); 3) Bovine rod outer segment (POS, Invision Bioresources, cat#98740), 4 million OS/retina. Bovine POS were diluted in serum-free DMEM/F12 (1:1; Gibco) to a concentration of 10^6 segments/ml and fluorescently labeled with the lipophilic dye DiI (Vybrant Cell-Labeling Solutions; Invitrogen) according to the manufacturer's instructions. Labeled $1x10^5$ POSs and 2mg/ml pHrodo™ Red E. coli membrane BioParticles and pHrodo™ Red Zymosan Bioparticles will be used for determining cell phagocytosis.

Harvested floating myeloid cells were transferred into 4-chamber slides to continue the culture. At the next day some chamber slides with myeloid cells were treated with three bioparticles and other slide chambers were continued culture with microglia cell differentiation for two weeks then treated with the three particles. The particles were added to the 100ul serum-free DMEM/F12 medium in the slide chamber respectively, incubated for one hour at 37°C and then washed with PBS 3 times, fixed with 4% paraformaldehyde (PFA) for 20 minutes, and went to staining further with IBa1, anti-human P2ry12 antibodies and DAPI. After staining, the slides were mounted with a mounting solution, and take images with Olympus 1000 confocal microscope. The bioparticles internalized cells, and the total cell number was counted using Image J software.

LPS challenge and pro-inflammatory factors assay

Differentiated hiPSC-derived microglia cells in 6-Well plates were stimulated with LPS at 100 ng/mL for 6 and 24 hr. The cells with LPS treated for 6 hrs were collected in RNA later solution and stored at -80°C for further QPCR analysis. The cells and medium with LPS treated for 24 hrs were collected for protein assay. After the medium was collected, the cells in the well were washed with 1XPBS, and then 200ul of RIPA lysis buffer with proteinase inhibitor cocktail (Calbiochem) was added; the cells were scratched with the cell scraper and collected into 1.5ml Eppendorf tube, homogenized using the sonicator (Sonicator 125 Watts, Qsonica) at 4°C. After sonication and centrifugation, protein concentration was measured (BCA protein assay kit; Pierce). Cytokine levels were determined using a Milliplex bead assay kit (Milliplex MAP human cytokine/chemokine magnetic bead panel, #MCYTOMAG-70K; Millipore) using the Luminex MAPIX system with data analysis using xPONENT 4.2 software (Luminex). The cytokine beads comprise IL1a, IL1B, IL6, IL8, TNFa, CXCL10, CCL2, CCL3, CCL4, IL10.

mRNA expression analysis by quantitative RT-PCR

The mRNA expression was quantitated using quantitative reverse transcription-PCR (qRT-PCR). Harvested cells were lysed by trituration and homogenized using QIAshredder spin columns (Qiagen). Total RNA was isolated using the RNeasy Mini kit (Qiagen) according to the manufacturer's specifications. First-strand cDNA synthesis from mRNA was performed using qScript cDNA SuperMix (Quanta Biosciences) using oligo-dT as primer. qRT-PCR was performed using an SYBR green RT-PCR kit (Affymetrix), using the Bio-Rad CFX96 Touch™ Real-Time PCR Detection System under the following conditions: denaturation at 95 °C for 5 min, followed by 40 cycles of 95 °C for 10 s, and then 60 °C for 45 s. Threshold cycle (CT) values were calculated and expressed as fold-induction determined using the comparative CT (2ΔΔCT) method. Ribosomal protein S13 (RPS13) and GAPDH were used as internal controls. Oligonucleotide primers are provided in Supplement Table 1.

hiPSC-derived microglia cells transplantation

The mature hiPSC-derived microglia cells in the flasks were washed with 1XPBS 1 time; after adding 5ml of 1XPBS, the cells were scratched by the cell scraper and collected into the 50ml tube. The cell number was counted by the cell counter (Countess 3, ThermoFisher). The cells were then centrifugated for 5 minutes at 4°C, 200g. The cell pellet was resuspended with 1XPBS as 5000/ul concentration. Subretinal injection of cells will be performed while the animal is still under anesthesia. Topical anesthesia (0.5% Proparacaine HCL, Sandoz) will be applied to the eye. The temporal side of the sclera will be exposed, and a puncture will be made at 0.5 mm behind the limbus with a sharp number 33 needle to reach the subretinal space. The tip of a blunt number 33 needle attached to a Hamilton micro-syringe will be introduced to the incision at a 5-degree angle toward the posterior pole (subretinal injection) and inserted 0.5-1 mm into the subretinal space under a dissecting microscope. The 1ul of the cells (5000 in PBS) will be slowly injected into the subretinal space. An aseptic technique will be used for the injection. Intraocular pressure post-procedure will be monitored by a tonometer and the globe will be carefully inspected for signs of bleeding or distention. If intraocular pressure is high (>20mmHg) and/or the globe appears distended, removal of a small volume of vitreous (about 1 microliter) using a 33-gauge needle will be performed to reduce intraocular pressure. In the unlikely event that excessive bleeding is observed, the animal will be examined by a veterinarian or euthanized immediately.

Immunocytochemistry staining on culture cells and retina

Harvested floating myeloid cells were transferred into 4-chamber slides to continue the culture. The next day, some chamber slides with myeloid cells were fixed; some slide chambers were continued culture with microglia cell differentiation for 2 weeks, then fixed with 4% PFA for 20 minutes and went to immunostaining. Mice were euthanized by CO2 inhalation, and their eyes were removed. Enucleated eyes were dissected to form posterior segment eyecups and fixed in 4% paraformaldehyde in phosphate buffer (PB) for 2 hr at 4°C. Eyecups were either cryosectioned (Leica CM3050S) or dissected to form retinal flat mounts. Flat-mounted retinas were blocked for 1 hr in a blocking buffer containing 10% normal donkey serum and 1% Triton X-100 in PBS at room temperature. Primary antibodies included IBA1 (1:500, Wako, #019–19741), anti-mouse TMEM119 (1:500, Synaptic Systems, #400 004), anti-human TMEM119 (1:100, Sigma, #HPA051870), anti-mouse CD68(1:200, BioRad, #MCA1957), anti-human CD68 (1:100, R&D, #MAB20401), anti-mouse CD45 (1:100, Bio-Rad, #MCA1388), anti-human CD45 (1:100, R&D, #FAB1430R), cone arrestin (1:200, Millipore, #AB15282), Ki67 (1:30, eBioscience, #50-5698-82), anti-P2RY12 (1:100, ThermoFisher, #PA5-77671 and Sigma, #HPA014518), CD34 (1:50, eBioscience, #14-0341), hCD11b (1:100, R&D, #FAB1699R), mCD11b (BioRad, Cat#: MCA711G, 1:100), CX3CR1 (1:100, Invitrogen, #61-6099-42), hHLA (Invitrogen, #11-9983-42), PU.1 (Invitrogen, #MA5-15064), Trem2 (1:100, Invitrogen, #702886), glutamine synthetase (1:200, Millipore, #MAB302), PKCa (1:200, Sigma-Aldrich, #p4334), GFAP (1:200, Invitrogen, #13–0300), RBPMS (1:100, Phosphosolutions, 1832-RBPMS), Calbindin (1:5000, Swant, CB-38a), and anti-RFP(1:200, RockLand, 600-401-379-RTU) were diluted in blocking buffer and applied overnight for sections and flat-mounts at room temperature on a shaker. Experiments in which primary antibodies were omitted served as negative controls. After washing in 1xPBST (0.2% Tween-20 in PBS), retinal samples were incubated for 2 hrs at room temperature with secondary antibodies (AlexaFluor 488-, 568- or 647-conjugated anti-rabbit, mouse, rat, goat and guinea pig IgG) and DAPI (1:500; Sigma-Aldrich) to label cell nuclei. Isolectin B4 (IB4), conjugated to AlexaFluor 568/647 (1:100, Life Technologies), was used to label activated microglia and retinal vessels. Stained retinal samples were imaged with confocal microscopy (Olympus FluoView 1000, or Zeiss LSM 880, or Nikon A1R). For analysis at high magnification, multiplane z-series were collected

using 20 or 40 objectives; Confocal image stacks were viewed and analyzed with FV100 Viewer Software, NIS-Element Analysis and Image J (NIH).

RNA seq and analysis

For whole transcriptome analysis, cultured MPC and mature differentiated microglia cells with and without 0.1ug/ml LPS treatment were harvested in the flasks and 6-well plates, respectively. After harvesting, all samples were frozen in RNA later (Roche) solution. The RNA extraction was done by the Qiagen RNA Mini Kit. RNA quality and quantity were evaluated using Bioanalyzer 2100 with the RNA 6000 Nano Kit (Agilent Technologies). The preparation of RNA library and transcriptome sequencing was conducted by Novogene Co., LTD (Califonia). Genes with adjusted p-value <0.05 and log2FC (FoldChange) > 1 were considered differentially expressed. IPA was employed for canonical pathway and graphic pathway analysis. The microglia gene list was constructed from our previous microarray data from retinal microglia cells (Ma et al. 2013; Bennett et al., 2016). The heat map, volcano, and histogram plot were performed with Prism 9.5.1 (Graph-Pad).

RPE cell damage model with sodium iodate (NaIO3)

In the NaIO3-induced RPE cells injury model, the Rag2−/−;Il2rg-/-;hCSF1+/+ mice after subretinal hiPSC-microglia cell transplantation for 8 months were administered a single dose of NaIO3 (Honeywell Research Chemicals) 30 mg/kg body weight via intraperitoneal injection. Animals were euthanized, and their retinas were analyzed at 3 and 7 days after NaIO3 injection.

Statistics and reproducibility

All data represent mean ± s.e.m. When only two independent groups were compared, significance was determined by a two-tailed unpaired t-test with Welch's correction. When three or more groups were compared, one-way ANOVA with the Bonferroni post hoc test or two-way ANOVA was used. A P value <0.05 was considered significant. The analyses were done in GraphPad Prism v.5. All experiments were independently performed at least three times with similar results.

SUPPLEMENTAL INFORMATION

Supplemental Information includes supplemental figures, tables, and key resources.

AUTHOR CONTRIBUTIONS

Wenxin Ma, performed and analyzed data and wrote the manuscript; Wai Wong and Wei Li designed and supervised the studies and edited the manuscript. Lian Zhao and Biying Xu did the injection, Robert N. Fariss helped with the image collection, Michael Redmond supervised and supported the study, and Juzhong Zou provided the hiPSC lines and iPSC quality control.

ACKNOWLEDGMENTS

This study was supported by the National Eye Institute Intramural Research program.

References

Abud EM, Ramirez RN, Martinez ES, Healy LM, Nguyen CHH, Newman SA, Yeromin AV, Scarfone VM, Marsh SE, Fimbres C, Caraway CA, Fote GM, Madany AM, Agrawal A, Kayed R, Gylys KH, Cahalan MD, Cummings BJ, Antel JP, Mortazavi A, Carson MJ, Poon WW, Blurton-Jones M. iPSC-Derived Human Microglia-like Cells to Study Neurological Diseases. Neuron. 2017 Apr 19;94(2):278-293.e9. doi: 10.1016/j.neuron.2017.03.042. PMID: 28426964; PMCID: PMC5482419.

Anderson SR, Roberts JM, Zhang J, Steele MR, Romero CO, Bosco A, et al. Developmental apoptosis promotes a disease-related gene signature and Independence from CSF1R signaling in retinal microglia. Cell Rep. 2019; 27(7):2002–13 e5.

Au NPB, Ma CHE. Neuroinflammation, Microglia and Implications for Retinal Ganglion Cell Survival and Axon Regeneration in Traumatic Optic Neuropathy. Front Immunol. 2022 Mar 4;13:860070. doi: 10.3389/fimmu.2022.860070. PMID: 35309305; PMCID: PMC8931466.

Beutner C, Lepperhof V, Dann A, Linnartz-Gerlach B, Litwak S, Napoli I, Prinz M, Neumann H. Engineered stem cell-derived microglia as therapeutic vehicle for experimental autoimmune encephalomyelitis. Gene Ther. 2013 Aug;20(8):797-806. doi: 10.1038/gt.2012.100. Epub 2013 Jan 17. PMID: 23324824.

Bohlen CJ, Bennett FC, Tucker AF, Collins HY, Mulinyawe SB, & Barres BA (2017). Diverse requirements for microglial survival, specification, and function revealed by defined-medium cultures. Neuron, 94(4), 759–773. 10.1016/j.neuron.2017.04.043 [PubMed: 28521131]

Bosco, A., Anderson, S. R., Roberts, J. M., Romero, C. O., Steele, M. R., and Vetter, M. L. (2019). Retinal microglia acquire a disease-associated transcriptome in chronic mouse glaucoma, which intensifies with neuroprotective complement inhibition. Invest. Ophthalmol. Vis. Sci. 60, 4002–4002.

Broderick C, Hoek RM, Forrester JV, Liversidge J, Sedgwick JD, Dick AD. Constitutive retinal CD200 expression regulates resident microglia and activation state of inflammatory cells during experimental autoimmune uveoretinitis. Am J Pathol. 2002 Nov;161(5):1669-77. doi: 10.1016/S0002-9440(10)64444-6. PMID: 12414514; PMCID: PMC1850781.

Burns TC, Li MD, Mehta S, Awad AJ, & Morgan AA (2015). Mouse models rarely mimic the transcriptome of human neurodegenerative diseases: A systematic bioinformatics-based critique of preclinical models. European Journal of Pharmacology, 759, 101–117. 10.1016/j.ejphar.2015.03.021 [PubMed: 25814260].

Butovsky O, Jedrychowski MP, Moore CS, Cialic R, Lanser AJ, Gabriely G, Koeglsperger T, Dake B, Wu PM, Doykan CE, Fanek Z, Liu L, Chen Z, Rothstein JD, Ransohoff RM, Gygi SP, Antel JP, Weiner HL. Identification of a unique TGF-β-dependent molecular and functional signature in microglia. Nat Neurosci. 2014 Jan;17(1):131-43. doi: 10.1038/nn.3599. Epub 2013 Dec 8. Erratum in: Nat Neurosci. 2014 Sep;17(9):1286. PMID: 24316888; PMCID: PMC4066672.

Chadarevian JP, Lombroso SI, Peet GC, Hasselmann J, Tu C, Marzan DE, Capocchi J, Purnell FS, Nemec KM, Lahian A, Escobar A, England W, Chaluvadi S, O'Brien CA, Yaqoob F, Aisenberg WH, Porras-Paniagua M, Bennett ML, Davtyan H, Spitale RC, Blurton-Jones M, Bennett FC. Engineering an inhibitor-resistant human CSF1R variant for microglia replacement. J Exp Med. 2023 Mar 6;220(3):e20220857. doi: 10.1084/jem.20220857. Epub 2022 Dec 30. PMID: 36584406; PMCID: PMC9814156.

Checchin D, Sennlaub F, Levavasseur E, Leduc M, Chemtob S. Potential role of microglia in retinal blood vessel formation. Invest Ophthalmol Vis Sci. 2006;47(8):3595–602.

Colonna M, Butovsky O. Microglia function in the central nervous system during health and Neurodegeneration. Annu Rev Immunol. 2017;35:441–68. 4.

Combadière, C., Feumi, C., Raoul, W., Keller, N., Rodéro, M., Pézard, A., et al. (2007). CX3CR1-dependent subretinal microglia cell accumulation is associated with cardinal features of age-related macular degeneration. J. Clin. Invest. 117, 2920–2928. doi: 10.1172/JCI31692.

Cukras CA, Petrou P, Chew EY, Meyerle CB, Wong WT. Oral minocycline for the treatment of diabetic macular edema (DME): results of a phase I/II clinical study. Invest Ophthalmol Vis Sci. 2012 Jun 22;53(7):3865-74. doi: 10.1167/iovs.11-9413. PMID: 22589436; PMCID: PMC3390218.

Dagher NN, Najafi AR, Kayala KM, Elmore MR, White TE, Medeiros R, West BL, Green KN. Colony-stimulating factor 1 receptor inhibition prevents microglial plaque association and improves cognition in 3xTg-AD mice. J Neuroinflammation. 2015 Aug 1;12:139. doi: 10.1186/s12974-015-0366-9. PMID: 26232154; PMCID: PMC4522109.

Dawson TM, Golde TE, & Lagier-Tourenne C (2018). Animal models of neurodegenerative diseases. Nature Neuroscience, 21(10), 1370–1379. 10.1038/s41593-018-0236-8 [PubMed: 30250265]

Den Hollander AI, Mullins RF, Orozco LD, Voigt AP, Chen HH, Strunz T, Grassmann F, Haines JL, Kuiper JJW, Tumminia SJ, Allikmets R, Hageman GS, Stambolian D, Klaver CCW, Boeke JD, Chen H, Honigberg L, Katti S, Frazer KA, Weber BHF, Gorin MB. Systems genomics in age-related macular degeneration. Exp Eye Res. 2022 Dec;225:109248. doi: 10.1016/j.exer.2022.109248. Epub 2022 Sep 13. PMID: 36108770; PMCID: PMC10150562.

Douvaras P, Sun B, Wang M, Kruglikov I, Lallos G, Zimmer M, Terrenoire C, Zhang B, Gandy S, Schadt E, Freytes DO, Noggle S, Fossati V. Directed Differentiation of Human Pluripotent Stem Cells to Microglia. Stem Cell Reports. 2017 Jun 6;8(6):1516-1524. doi: 10.1016/j.stemcr.2017.04.023. Epub 2017 May 18. PMID: 28528700; PMCID: PMC5470097.

Elmore MRP, Hohsfield LA, Kramár EA, Soreq L, Lee RJ, Pham ST, Najafi AR, Spangenberg EE, Wood MA, West BL, Green KN. Replacement of microglia in the aged brain reverses cognitive, synaptic, and neuronal deficits in mice. Aging Cell. 2018 Dec;17(6):e12832. doi: 10.1111/acel.12832. Epub 2018 Oct 2. PMID: 30276955; PMCID: PMC6260908.

Friedman BA, Srinivasan K, Ayalon G, Meilandt WJ, Lin H, Huntley MA, Cao Y, Lee SH, Haddick PCG, Ngu H, Modrusan Z, Larson JL, Kaminker JS, van der Brug MP, Hansen DV. Diverse Brain Myeloid Expression Profiles Reveal Distinct Microglial Activation States and Aspects of Alzheimer's Disease Not Evident in Mouse Models. Cell Rep. 2018 Jan 16;22(3):832-847. doi: 10.1016/j.celrep.2017.12.066. PMID: 29346778.

Fritsche LG, Igl W, Bailey JN, Grassmann F, … Weber BH, Abecasis GR, Heid IM. A large genome-wide association study of age-related macular degeneration highlights contributions of rare and common variants. Nat Genet. 2016 Feb;48(2):134-43. doi: 10.1038/ng.3448. Epub 2015 Dec 21. PMID: 26691988; PMCID: PMC4745342.

Galatro TF, Holtman IR, Lerario AM, Vainchtein ID, Brouwer N, Sola PR, Veras MM, Pereira TF, Leite REP, Möller T, Wes PD, Sogayar MC, Laman JD, den Dunnen W, Pasqualucci CA, Oba-Shinjo SM, Boddeke EWGM, Marie SKN, Eggen BJL. Transcriptomic analysis of purified human cortical microglia reveals age-associated changes. Nat Neurosci. 2017 Aug;20(8):1162-1171. doi: 10.1038/nn.4597. Epub 2017 Jul 3. PMID: 28671693.

Gao ML, Zhang X, Han F, Xu J, Yu SJ, Jin K, Jin ZB. Functional microglia derived from human pluripotent stem cells empower retinal organ. Sci China Life Sci. 2022 Jun;65(6):1057-1071. doi: 10.1007/s11427-021-2086-0. Epub 2022 Apr 22. PMID: 35451725.

Gosselin D, Skola D, Coufal NG, Holtman IR, Schlachetzki JCM, Sajti E, Jaeger BN, O'Connor C, Fitzpatrick C, Pasillas MP, Pena M, Adair A, Gonda DD, Levy ML, Ransohoff RM, Gage FH, Glass CK. An environment-dependent transcriptional network specifies human microglia identity. Science. 2017 Jun 23;356(6344):eaal3222. doi: 10.1126/science.aal3222. Epub 2017 May 25. PMID: 28546318; PMCID: PMC5858585.

Green, D. R., Oguin, T. H., and Martinez, J. (2016). The clearance of dying cells: table for two. Cell Death Differ. 23, 915–926. doi: 10.1038/cdd.2015.172.

Guilliams M, Scott CL. Does niche competition determine the origin of tissue-resident macrophages? Nat Rev Immunol. 2017 Jul;17(7):451-460. doi: 10.1038/nri.2017.42. Epub 2017 May 2. PMID: 28461703.

Guo S, Cázarez-Márquez F, Jiao H, Foppen E, Korpel NL, Grootemaat AE, Liv N, Gao Y, van der Wel N, Zhou B, Nie G, Yi CX. Specific Silencing of Microglial Gene Expression in the Rat Brain by Nanoparticle-Based Small Interfering RNA Delivery. ACS Appl Mater Interfaces. 2022 Feb 2;14(4):5066-5079. doi: 10.1021/acsami.1c22434. Epub 2022 Jan 18. PMID: 35041392; PMCID: PMC8815040.

Haenseler W, Sansom SN, Buchrieser J, Newey SE, Moore CS, Nicholls FJ, Chintawar S, Schnell C, Antel JP, Allen ND, Cader MZ, Wade-Martins R, James WS, Cowley SA. A Highly Efficient Human Pluripotent Stem Cell Microglia Model Displays a Neuronal-Co-culture-Specific Expression Profile and Inflammatory Response. Stem Cell Reports. 2017 Jun 6;8(6):1727-1742. doi: 10.1016/j.stemcr.2017.05.017. PMID: 28591653; PMCID: PMC5470330.

Han J, Sarlus H, Wszolek ZK, Karrenbauer VD, Harris RA. Microglial replacement therapy: a potential therapeutic strategy for incurable CSF1R-related leukoencephalopathy. Acta Neuropathol Commun. 2020 Dec 7;8(1):217. doi: 10.1186/s40478-020-01093-3. PMID: 33287883; PMCID: PMC7720517.

Hasselmann J, Blurton-Jones M. Human iPSC-derived microglia: A growing toolset to study the brain's innate immune cells. Glia. 2020 Apr;68(4):721-739. doi: 10.1002/glia.23781. Epub 2020 Jan 11. PMID: 31926038; PMCID: PMC7813153.

Hohsfield LA, Najafi AR, Ghorbanian Y, Soni N, Hingco EE, Kim SJ, Jue AD, Swarup V, Inlay MA, Green KN. Effects of long-term and brain-wide colonization of peripheral bone marrow-derived myeloid cells in the CNS. J Neuroinflammation. 2020 Sep 20;17(1):279. doi: 10.1186/s12974-020-01931-0. PMID: 32951604; PMCID: PMC7504855.

Hong S, Dissing-Olesen L, Stevens B. New insights on the role of microglia in synaptic pruning in health and disease. Curr Opin Neurobiol. 2016;36: 128 –34.

Huang T, Cui J, Li L, Hitchcock PF, Li Y. The role of microglia in the neurogenesis of zebrafish retina. Biochem Biophys Res Commun. 2012; 421(2):214 –20

Huang Y, Xu Z, Xiong S, Qin G, Sun F, Yang J, Yuan TF, Zhao L, Wang K, Liang YX, Fu L, Wu T, So KF, Rao Y, Peng B. Dual extra-retinal origins of microglia in the model of retinal microglia repopulation. Cell Discov. 2018 Feb 27;4:9. doi: 10.1038/s41421-018-0011-8. PMID: 29507754; PMCID: PMC5827656.

Karlsson KR, Cowley S, Martinez FO, Shaw M, Minger SL, James W. Homogeneous monocytes and macrophages from human embryonic stem cells following coculture-free differentiation in M-CSF and IL-3. Exp Hematol. 2008 Sep;36(9):1167-75. doi: 10.1016/j.exphem.2008.04.009. Epub 2008 Jun 11. PMID: 18550257; PMCID: PMC2635571.

Karlstetter M, Scholz R, Rutar M, Wong WT, Provis JM, Langmann T. Retinal microglia: just bystander or target for therapy? Prog Retin Eye Res. 2015 Mar;45:30-57. doi: 10.1016/j.preteyeres.2014.11.004. Epub 2014 Dec 2. PMID: 25476242.

Kubota Y, Takubo K, Shimizu T, Ohno H, Kishi K, Shibuya M, et al. M-CSF inhibition selectively targets pathological angiogenesis and lymphangiogenesis. J Exp Med. 2009;206(5):1089–102

Larochelle A, Bellavance MA, Michaud JP, Rivest S. Bone marrow-derived macrophages and the CNS: An update on the use of experimental chimeric mouse models and bone marrow transplantation in neurological disorders. Biochim Biophys Acta. 2016 Mar;1862(3):310-22. doi: 10.1016/j.bbadis.2015.09.017. Epub 2015 Oct 8. PMID: 26432480.

Leach LL, Croze RH, Hu Q, Nadar VP, Clevenger TN, Pennington BO, Gamm DM, Clegg DO. Induced Pluripotent Stem Cell-Derived Retinal Pigmented Epithelium: A Comparative Study Between Cell Lines and Differentiation Methods. J Ocul Pharmacol Ther. 2016 Jun;32(5):317-30. doi: 10.1089/jop.2016.0022. Epub 2016 May 16. PMID: 27182743; PMCID: PMC5911695.

Lee JE, Liang KJ, Fariss RN, Wong WT. Ex vivo dynamic imaging of retinal microglia using time-lapse confocal microscopy. Invest Ophthalmol Vis Sci. 2008 Sep;49(9):4169-76. doi: 10.1167/iovs.08-2076. Epub 2008 May 16. PMID: 18487378; PMCID: PMC2652634.

Li Q, Barres BA. Microglia and macrophages in brain homeostasis and disease. Nat Rev Immunol. 2018;18(4):225–42. 3.

Lund H, Pieber M, Parsa R, Han J, Grommisch D, Ewing E, Kular L, Needhamsen M, Espinosa A, Nilsson E, Överby AK, Butovsky O, Jagodic M, Zhang XM, Harris RA. Competitive repopulation of an empty microglial niche yields functionally distinct subsets of microglia-like cells. Nat Commun. 2018 Nov 19;9(1):4845. doi: 10.1038/s41467-018-07295-7. PMID: 30451869; PMCID: PMC6242869.

Ma W, Cojocaru R, Gotoh N, Gieser L, Villasmil R, Cogliati T, Swaroop A, Wong WT. Gene expression changes in aging retinal microglia: relationship to microglial support functions and regulation of activation. Neurobiol Aging. 2013 Oct;34(10):2310-21. doi: 10.1016/j.neurobiolaging.2013.03.022. Epub 2013 Apr 19. PMID: 23608111; PMCID: PMC3706521.

Ma W, Zhang Y, Gao C, Fariss RN, Tam J, Wong WT. Monocyte infiltration and proliferation reestablish myeloid cell homeostasis in the mouse retina following retinal pigment epithelial cell injury. Sci Rep. 2017 Aug 16;7(1):8433. doi: 10.1038/s41598-017-08702-7. PMID: 28814744; PMCID: PMC5559448.

Ma W, Zhao L, Fontainhas AM, Fariss RN, Wong WT. Microglia in the mouse retina alter the structure and function of retinal pigmented epithelial cells: a potential cellular interaction relevant to AMD. PLoS One. 2009 Nov 20;4(11):e7945. doi: 10.1371/journal.pone.0007945. PMID: 19936204; PMCID: PMC2775955.

Ma W, Zhao L, Fontainhas AM, Fariss RN, Wong WT. Microglia in the mouse retina alter the structure and function of retinal pigmented epithelial cells: a potential cellular interaction relevant to AMD. PLoS One. 2009 Nov 20;4(11):e7945. doi: 10.1371/journal.pone.0007945. PMID: 19936204; PMCID: PMC2775955.

Ma W, Zhao L, Wong WT. Microglia in the outer retina and their relevance to pathogenesis of age-related macular degeneration. Adv Exp Med Biol. 2012;723:37-42. doi:10.1007/978-1-4614-0631-0_6

Mancuso R, Van Den Daele J, Fattorelli N, Wolfs L, Balusu S, Burton O, Liston A, Sierksma A, Fourne Y, Poovathingal S, Arranz-Mendiguren A, Sala Frigerio C, Claes C, Serneels L, Theys T, Perry VH, Verfaillie C, Fiers M, De Strooper B. Stem-cell-derived human microglia transplanted in mouse brain to study human disease. Nat Neurosci. 2019 Dec;22(12):2111-2116. doi: 10.1038/s41593-019-0525-x. Epub 2019 Oct 28. PMID: 31659342.

Muffat J, Li Y, Yuan B, Mitalipova M, Omer A, Corcoran S, Bakiasi G, Tsai LH, Aubourg P, Ransohoff RM, Jaenisch R. Efficient derivation of microglia-like cells from human pluripotent stem cells. Nat Med. 2016 Nov;22(11):1358-1367. doi: 10.1038/nm.4189. Epub 2016 Sep 26. PMID: 27668937; PMCID: PMC5101156.

Nau R, Ribes S, Djukic M, Eiffert H. Strategies to increase the activity of microglia as efficient protectors of the brain against infections. Front Cell Neurosci. 2014 May 22;8:138. doi: 10.3389/fncel.2014.00138. PMID: 24904283; PMCID: PMC4033068.

Neumann H. Microglia: a cellular vehicle for CNS gene therapy. J Clin Invest. 2006 Nov;116(11):2857-60. doi: 10.1172/JCI30230. PMID: 17080190; PMCID: PMC1626126.

Okunuki Y, Mukai R, Nakao T, Tabor SJ, Butovsky O, Dana R, Ksander DR, Connor KM. Retinal microglia initiate neuroinflammation in ocular autoimmunity. PNAS, 2019, 116 (20) 9989-9998; DOI: 10.1073/pnas.1820387116

Pandya H, Shen MJ, Ichikawa DM, Sedlock AB, Choi Y, Johnson KR, Kim G, Brown MA, Elkahloun AG, Maric D, Sweeney CL, Gossa S, Malech HL, McGavern DB, Park JK. Differentiation of human and murine induced pluripotent stem cells to microglia-like cells. Nat Neurosci. 2017 May;20(5):753-759. doi: 10.1038/nn.4534. Epub 2017 Mar 2. PMID: 28253233; PMCID: PMC5404968.

Paolicelli RC, Bolasco G, Pagani F, Maggi L, Scianni M, Panzanelli P, Giustetto M, Ferreira TA, Guiducci E, Dumas L, Ragozzino D, Gross CT. Synaptic pruning by microglia is necessary for normal brain development. Science. 2011 Sep 9;333(6048):1456-8. doi: 10.1126/science.1202529. Epub 2011 Jul 21. PMID: 21778362.

Parajuli B, Saito H, Shinozaki Y, Shigetomi E, Miwa H, Yoneda S, Tanimura M, Omachi S, Asaki T, Takahashi K, Fujita M, Nakashima K, Koizumi S. Transnasal transplantation of human induced pluripotent stem cell-derived microglia to the brain of immunocompetent mice. Glia. 2021 Oct;69(10):2332-2348. doi: 10.1002/glia.23985. Epub 2021 Jul 26. PMID: 34309082.

Pocock JM, Piers TM. Modelling microglial function with induced pluripotent stem cells: an update. Nat Rev Neurosci. 2018 Aug;19(8):445-452. doi: 10.1038/s41583-018-0030-3. PMID: 29977068.

Puñal V, Paisley C, Brecha F, Lee M, Perelli R, Wang J et al. Large-scale death of retinal astrocytes during normal development is non-apoptotic and implemented by microglia. PLoS Biology, 2019:17(10).

Ramírez AI, de Hoz R, Fernández-Albarral JA, Salobrar-Garcia E, Rojas B, Valiente-Soriano FJ, Avilés-Trigueros M, Villegas-Pérez MP, Vidal-Sanz M, Triviño A, Ramírez JM, Salazar JJ. Time course of bilateral microglial activation in a mouse model of laser-induced glaucoma. Sci Rep. 2020 Mar 17;10(1):4890. doi: 10.1038/s41598-020-61848-9. PMID: 32184450; PMCID: PMC7078298.

Réu P, Khosravi A, Bernard S, Mold JE, Salehpour M, Alkass K, Perl S, Tisdale J, Possnert G, Druid H, Frisén J. The Lifespan and Turnover of Microglia in the Human Brain. Cell Rep. 2017 Jul 25;20(4):779-784. doi: 10.1016/j.celrep.2017.07.004. PMID: 28746864; PMCID: PMC5540680.

Ritter MR, Banin E, Moreno SK, Aguilar E, Dorrell MI, Friedlander M. Myeloid progenitors differentiate into microglia and promote vascular repair in a model of ischemic retinopathy. J Clin Invest. 2006;116(12):3266–76. 104.

Schafer DP, Lehrman EK, Kautzman AG, Koyama R, Mardinly AR, Yamasaki R, et al. Microglia sculpt postnatal neural circuits in an activity and complement-dependent manner. Neuron. 2012;74(4):691–705.

Schafer DP, Stevens B. Microglia function in central nervous system development and plasticity. Cold Spring Harb Perspect Biol. 2015;7(10): a020545. 133.

Shi Q, Chang C, Saliba A, Bhat MA. Microglial mTOR Activation Upregulates Trem2 and Enhances β-Amyloid Plaque Clearance in the 5XFAD Alzheimer's Disease Model. J Neurosci. 2022 Jul 6;42(27):5294-5313. doi: 10.1523/JNEUROSCI.2427-21.2022. Epub 2022 Jun 7. PMID: 35672148; PMCID: PMC9270922.

Shibuya Y, Kumar KK, Mader MM, Yoo Y, Ayala LA, Zhou M, Mohr MA, Neumayer G, Kumar I, Yamamoto R, Marcoux P, Liou B, Bennett FC, Nakauchi H, Sun Y, Chen X, Heppner FL, Wyss-Coray T, Südhof TC, Wernig M. Treatment of a genetic brain disease by CNS-wide microglia replacement. Sci Transl Med. 2022 Mar 16;14(636):eabl9945. doi: 10.1126/scitranslmed.abl9945. Epub 2022 Mar 16. PMID: 35294256; PMCID: PMC9618306.

Sierra A, Abiega O, Shahraz A, Neumann H. Janus-faced microglia: beneficial and detrimental consequences of microglial phagocytosis. Front Cell Neurosci. 2013;7:6.

Silverman SM, Ma W, Wang X, Zhao L, Wong WT. C3- and CR3-dependent microglial clearance protects photoreceptors in retinitis pigmentosa. J Exp Med. 2019 Aug 5;216(8):1925-1943. doi: 10.1084/jem.20190009. Epub 2019 Jun 17. PMID: 31209071; PMCID: PMC6683998.

Smith AM, & Dragunow M (2014). The human side of microglia. Trends in Neurosciences, 37(3), 125–135. 10.1016/j.tins.2013.12.001 [PubMed: 24388427]

Stevens B, Allen NJ, Vazquez LE, Howell GR, Christopherson KS, Nouri N, et al. The classical complement cascade mediates CNS synapse elimination. Cell. 2007;131(6):1164–78

Svoboda DS, Barrasa MI, Shu J, Rietjens R, Zhang S, Mitalipova M, Berube P, Fu D, Shultz LD, Bell GW, Jaenisch R. Human iPSC-derived microglia assume a primary microglia-like state after transplantation into the neonatal mouse brain. Proc Natl Acad Sci U S A. 2019 Dec 10;116(50):25293-25303. doi: 10.1073/pnas.1913541116. Epub 2019 Nov 26. PMID: 31772018; PMCID: PMC6911218.

Takata K, Kozaki T, Lee CZW, Thion MS, Otsuka M, Lim S, Utami KH, Fidan K, Park DS, Malleret B, Chakarov S, See P, Low D, Low G, Garcia-Miralles M, Zeng R, Zhang J, Goh CC, Gul A, Hubert S, Lee B, Chen J, Low I, Shadan NB, Lum J, Wei TS, Mok E, Kawanishi S, Kitamura Y, Larbi A, Poidinger M, Renia L, Ng LG, Wolf Y, Jung S, Önder T, Newell E, Huber T, Ashihara E, Garel S, Pouladi MA, Ginhoux F. Induced-Pluripotent-Stem-Cell-Derived Primitive Macrophages Provide a Platform for Modeling Tissue-Resident Macrophage Differentiation and Function. Immunity. 2017 Jul 18;47(1):183-198.e6. doi: 10.1016/j.immuni.2017.06.017. Erratum in: Immunity. 2020 Feb 18;52(2):417-418. PMID: 28723550.

Tanaka T, Yokoi T, Tamalu F, Watanabe S, Nishina S, Azuma N. Generation of Retinal Ganglion Cells With Functional Axons From Mouse Embryonic Stem Cells and Induced Pluripotent Stem Cells. Invest Ophthalmol Vis Sci. 2016 Jun 1;57(7):3348-59. doi: 10.1167/iovs.16-19166. PMID: 27367502.

Ueda Y, Gullipalli D, & Song WC (2016). Modeling complement-driven diseases in transgenic mice: Values and limitations. Immunobiology, 221(10), 1080–1090. 10.1016/j.imbio.2016.06.007 [PubMed: 27371974]

Ulland TK, Colonna M. TREM2 - a key player in microglial biology and Alzheimer disease. Nat Rev Neurol. 2018 Nov;14(11):667-675. doi: 10.1038/s41582-018-0072-1. PMID: 30266932.

Van Wilgenburg B, Browne C, Vowles J, Cowley SA. Efficient, long term production of monocyte-derived macrophages from human pluripotent stem cells under partly-defined and fully-defined conditions. PLoS One. 2013 Aug 12;8(8):e71098. doi: 10.1371/journal.pone.0071098. PMID: 23951090; PMCID: PMC3741356.

Wang S, Mustafa M, Yuede CM, Salazar SV, Kong P, Long H, Ward M, Siddiqui O, Paul R, Gilfillan S, Ibrahim A, Rhinn H, Tassi I, Rosenthal A, Schwabe T, Colonna M. Anti-human TREM2 induces microglia proliferation and reduces pathology in an Alzheimer's disease model. J Exp Med. 2020 Sep 7;217(9):e20200785. doi: 10.1084/jem.20200785. PMID: 32579671; PMCID: PMC7478730.

Wang X, Zhao L, Zhang J, Fariss RN, Ma W, Kretschmer F, Wang M, Qian HH, Badea TC, Diamond JS, Gan WB, Roger JE, Wong WT. Requirement for Microglia for the Maintenance of Synaptic Function and Integrity in the Mature Retina. J Neurosci. 2016 Mar 2;36(9):2827-42. doi: 10.1523/JNEUROSCI.3575-15.2016. PMID: 26937019; PMCID: PMC4879218.

Willis EF, MacDonald KPA, Nguyen QH, Garrido AL, Gillespie ER, Harley SBR, Bartlett PF, Schroder WA, Yates AG, Anthony DC, Rose-John S, Ruitenberg MJ, Vukovic J. Repopulating Microglia Promote Brain Repair in an IL-6-Dependent Manner. Cell. 2020 Mar 5;180(5):833-846.e16. doi: 10.1016/j.cell.2020.02.013. PMID: 32142677.

Xu H, Chen M, Diabetic retinopathy and dysregulated innate immunity, Vision Research, Volume 139, 2017, Pages 39-46, ISSN 0042-6989.

Xu R, Li X, Boreland AJ, Posyton A, Kwan K, Hart RP, Jiang P. Human iPSC-derived mature microglia retain their identity and functionally integrate in the chimeric mouse brain. Nat Commun. 2020 Mar 27;11(1):1577. doi: 10.1038/s41467-020-15411-9. PMID: 32221280; PMCID: PMC7101330.

Xu Z, Rao Y, Huang Y, Zhou T, Feng R, Xiong S, Yuan TF, Qin S, Lu Y, Zhou X, Li X, Qin B, Mao Y, Peng B. Efficient Strategies for Microglia Replacement in the Central Nervous System. Cell Rep. 2020 Nov 24;33(8):108443. doi: 10.1016/j.celrep.2020.108443. Erratum for: Cell Rep. 2020 Aug 11;32(6):108041. PMID: 33238120.

Zhang Y, Zhao L, Wang X, Ma W, Lazere A, Qian HH, Zhang J, Abu-Asab M, Fariss RN, Roger JE, Wong WT. Repopulating retinal microglia restore endogenous organization and function under CX3CL1-CX3CR1 regulation. Sci Adv. 2018 Mar 21;4(3):eaap8492. doi: 10.1126/sciadv.aap8492. PMID: 29750189; PMCID: PMC5943055.

Zhao L, Ma W, Fariss RN, Wong WT. Minocycline attenuates photoreceptor degeneration in a mouse model of subretinal hemorrhage microglial: inhibition as a potential therapeutic strategy. Am J Pathol. 2011 Sep;179(3):1265-77. doi: 10.1016/j.ajpath.2011.05.042. Epub 2011 Jul 19. PMID: 21763674; PMCID: PMC3157282.

Zhao L, Zabel MK, Wang X, Ma W, Shah P, Fariss RN, Qian H, Parkhurst CN, Gan WB, Wong WT. Microglial phagocytosis of living photoreceptors contributes to inherited retinal degeneration. EMBO Mol Med. 2015 Sep;7(9):1179-97. doi: 10.15252/emmm.201505298. PMID: 26139610; PMCID: PMC4568951.

Zhong X, Gutierrez C, Xue T, Hampton C, Vergara MN, Cao LH, Peters A, Park TS, Zambidis ET, Meyer JS, Gamm DM, Yau KW, Canto-Soler MV. Generation of three-dimensional retinal tissue with functional photoreceptors from human iPSCs. Nat Commun. 2014 Jun 10;5:4047. doi: 10.1038/ncomms5047. PMID: 24915161; PMCID: PMC4370190.

Zhou J, Yang J, Dai M, Lin D, Zhang R, Liu H, Yu A, Vakal S, Wang Y, Li X. A combination of inhibiting microglia activity and remodeling gut microenvironment suppresses the development and progression of experimental autoimmune uveitis. Biochem Pharmacol. 2020 Oct;180:114108. doi: 10.1016/j.bcp.2020.114108. Epub 2020 Jun 20. PMID: 32569628.

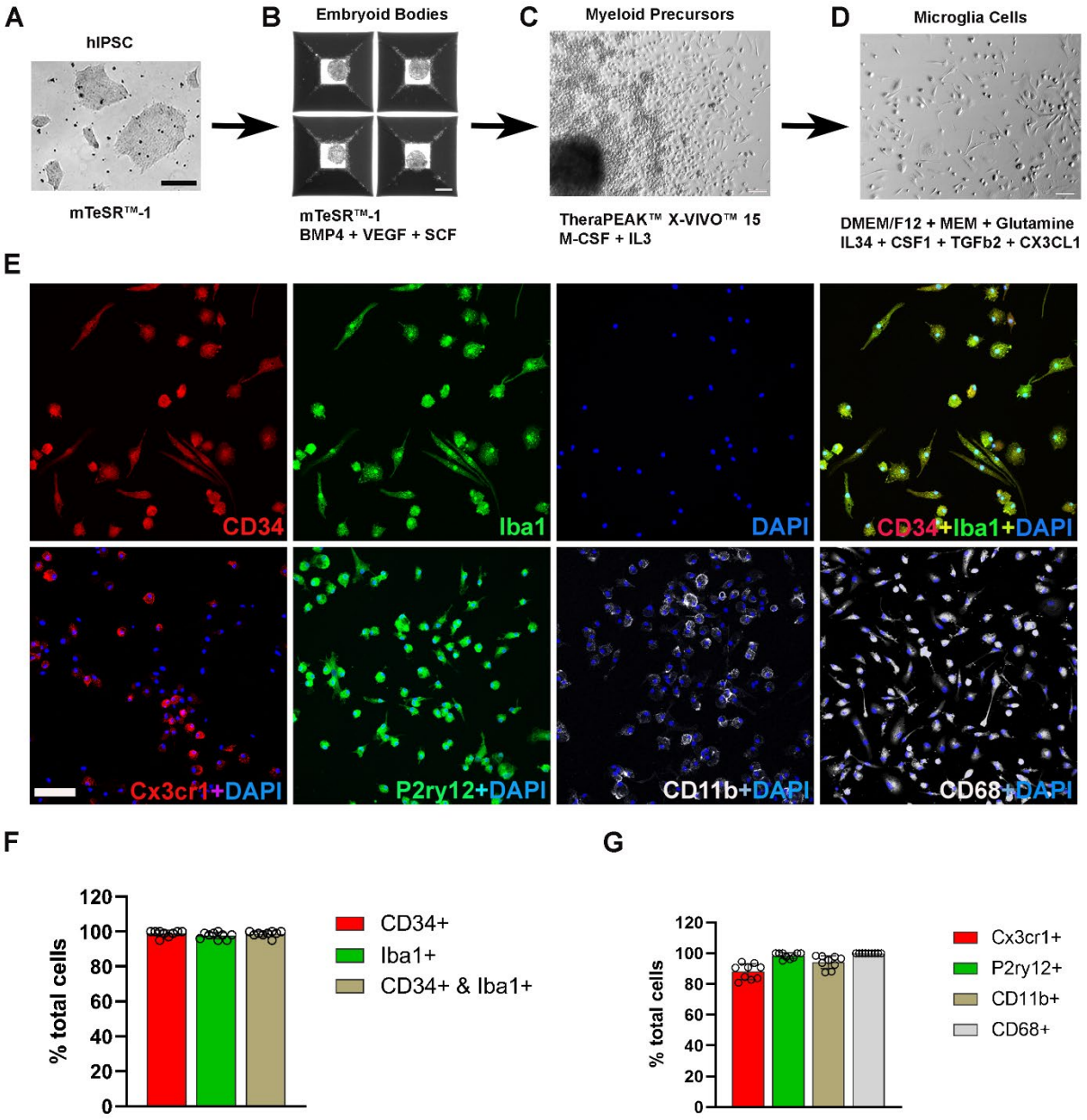

Figure 1. Differentiation and characterization of human iPSC-derived microglia cell. (A) Human iPSC were cultured in a 6-well plate. Scale bar = 200µm. (B) Embryoid bodies formation in AggreWell™800 plate at day eight in culture medium mTeSR1 plus BMP4, VEGF, and SCF. Scale bar = 200µm. (C) Myeloid precursor cluster at the 1-month culture of embryoid bodies under TheraPEAK™ X-vivo™-15 Serum-free Hematopoietic Cell Medium with M-CSF and IL3. Scale bar = 50µm. (D) Microglia cells maturation culture for two weeks with DMEM/F12 plus nonessential amino acids, glutamine, IL34, CSF1, TGFb2, and CX3CL1. Scale bar = 50µm. (E) Immunocytochemistry staining with Iba1 and human CD34, CX3CR1, P2ry12, CD11b, CD68. Scale bar = 100µm. (F) The cell counts and collaboration analysis of CD34 and Iba1 positive cells. (G) Percentage analysis of myeloid cell marker CX3CR1, CD11b, activation marker CD68, and microglia cell signature marker P2ry12.

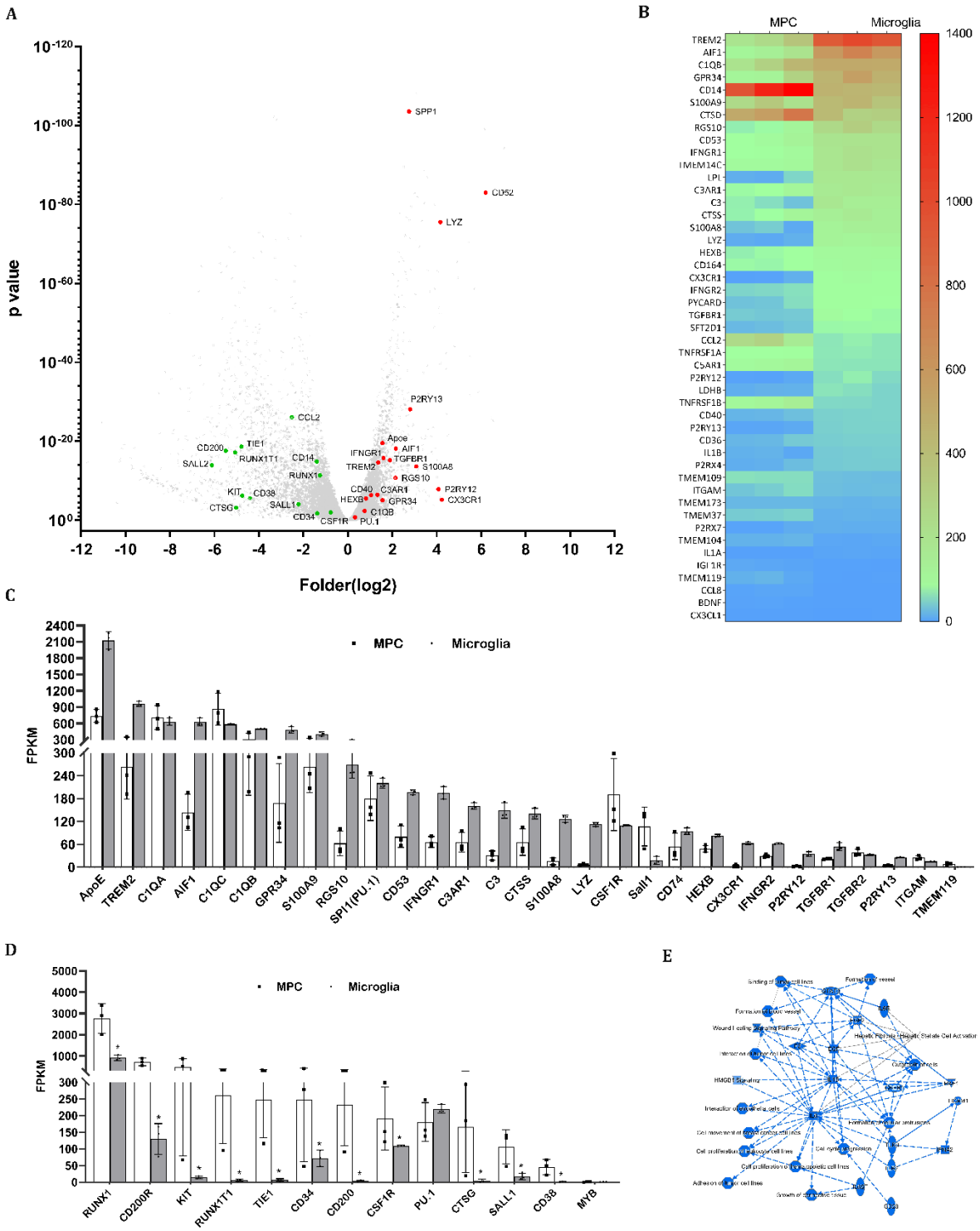

Figure 2. Comparison of the gene expression profile of mature microglia cells vs. myeloid progenitor cells (MPC) with bulk RNA seq. (A) The volcano plot shows the gene expression in mature human microglia cells and MPC. The MPC and microglia representative genes were showed in green and red color. (B) The heat map shows mature microglia-enrich gene expression compared to MPC. (C) Histogram showed the comparison of microglia-enrich gene expression in human iPSC-derived MPC and

microglia cells with FPKM. (D) Histogram showed the comparison of myeloid cell lineage gene expression in human iPSC-derived MPC and mature microglia cells with FPKM. (E) Graphic signaling pathway analysis with IPA showed the hub genes are IL6 and IL1b in comparison of mature microglia vs. myeloid progenitors.

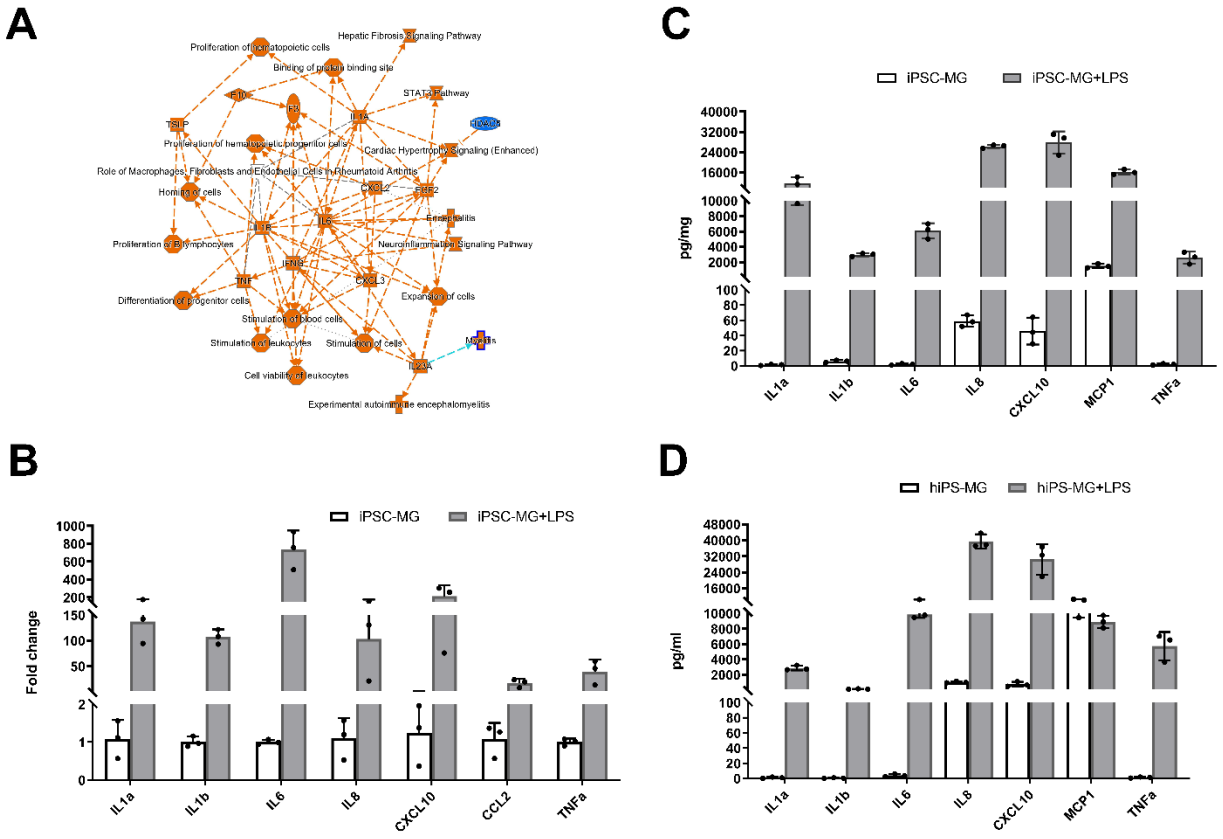

Figure 3. Inflammation responses of Human iPSC-derived microglia cells under Lipopolysaccharide (LPS) stimulation. (A) Graphic signaling pathway analysis with IPA on comparison of LPS-treated and non-LPS-treated microglia cells showed the increased core pathways are IL6, IL1a, IL1b, and IFNG. (B) The QPCR results showed proinflammatory factors expression increased after LPS (0.1ug/ml) stimulation for 6hrs. (C) The inflammatory cytokines in protein level without/with LPS (0.1ug/ml) stimulation for 24hrs in human iPSC-derived microglia cell lysate. (D) Human iPSC-derived microglia cells released inflammatory cytokines in the medium without/with LPS (0.1ug/ml) stimulation for 24hrs. (C) and (D) results were measured with a Multiplex kit (Millipore), Graphical data in (C) and (D) are presented as means ± SEM).

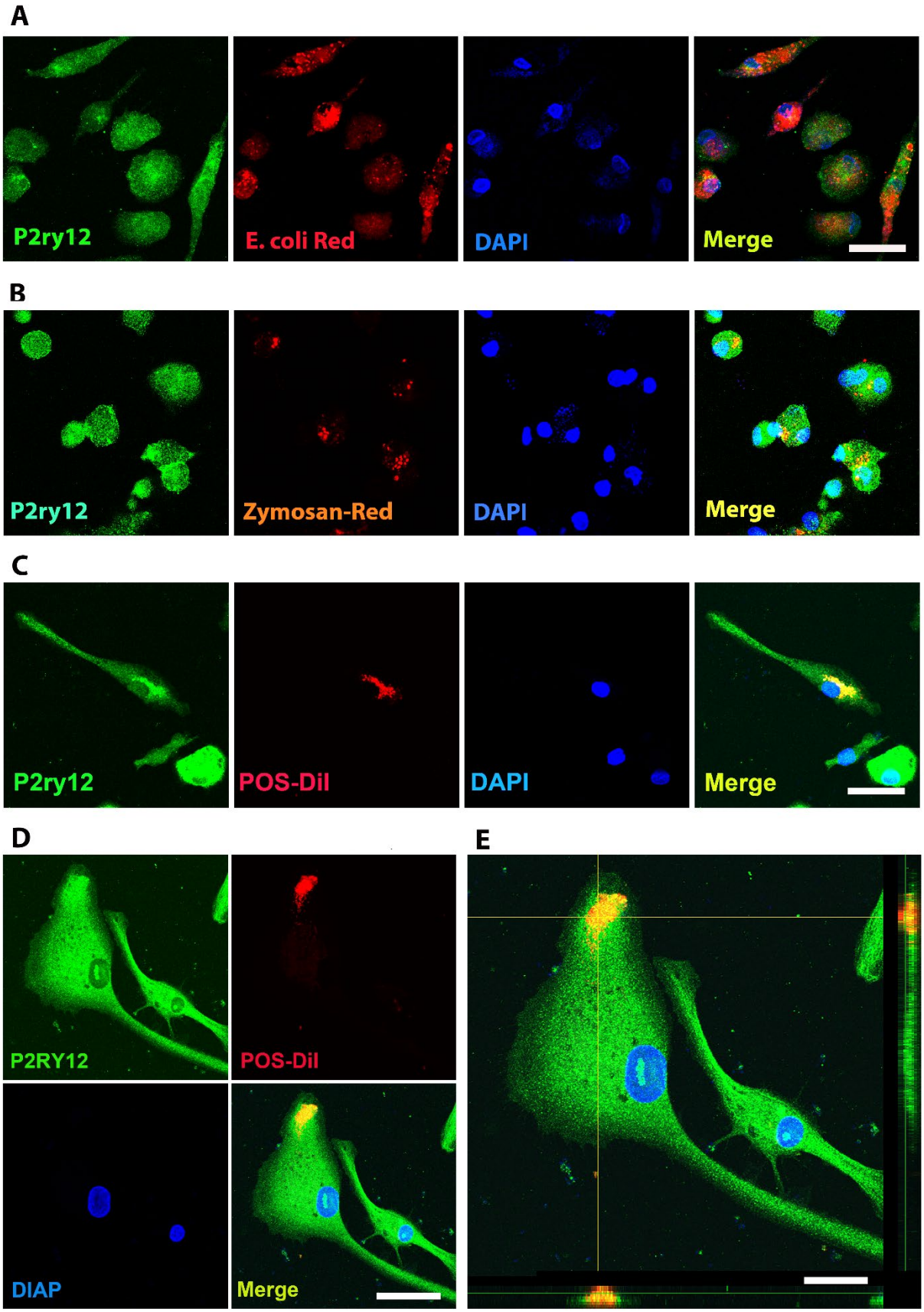
A
P2ry12
E. coli Red
DAPI
Merge
B
P2ry12
Zymosan-Red
DAPI
Merge
C
P2ry12
POS-DiI
DAPI
Merge
D
P2RY12
POS-DiI
DIAP
Merge
E

Figure 4. Phagocytosis evaluation of Human iPSC-derived microglia cells. (A) pHrodo™ Red E. coli Bioparticles were incubated in Human iPSC-derived microglia cells for 1 hour. After washing with PBS, Human iPSC-derived microglia cells were stained with anti-human P2ry12 antibody (green) and DAPI. Scale bar = 40µm. (B) pHrodo™ Red Zymosan Bioparticles were incubated in human iPSC-derived microglia cells for 1 hour. After washing with PBS, Human iPSC-derived microglia cells were stained with anti-human P2ry12 antibody (green) and DAPI. Scale bar = 40µm. (C) DiI (Vybrant Cell-Labeling Solutions; Invitrogen) labeled bovine photoreceptor outer segments (POS) were added to the culture medium and incubated for 1 hour. After washing with PBS, Human iPSC-derived microglia cells were stained with anti-human P2ry12 antibody (green) and DAPI. Scale bar = 40µm. (D) and (E) are highly magnificent showed of POS-DiI in human iPSC-derived microglia cells. Scale bar = 30µm (D) and 15µm (E).

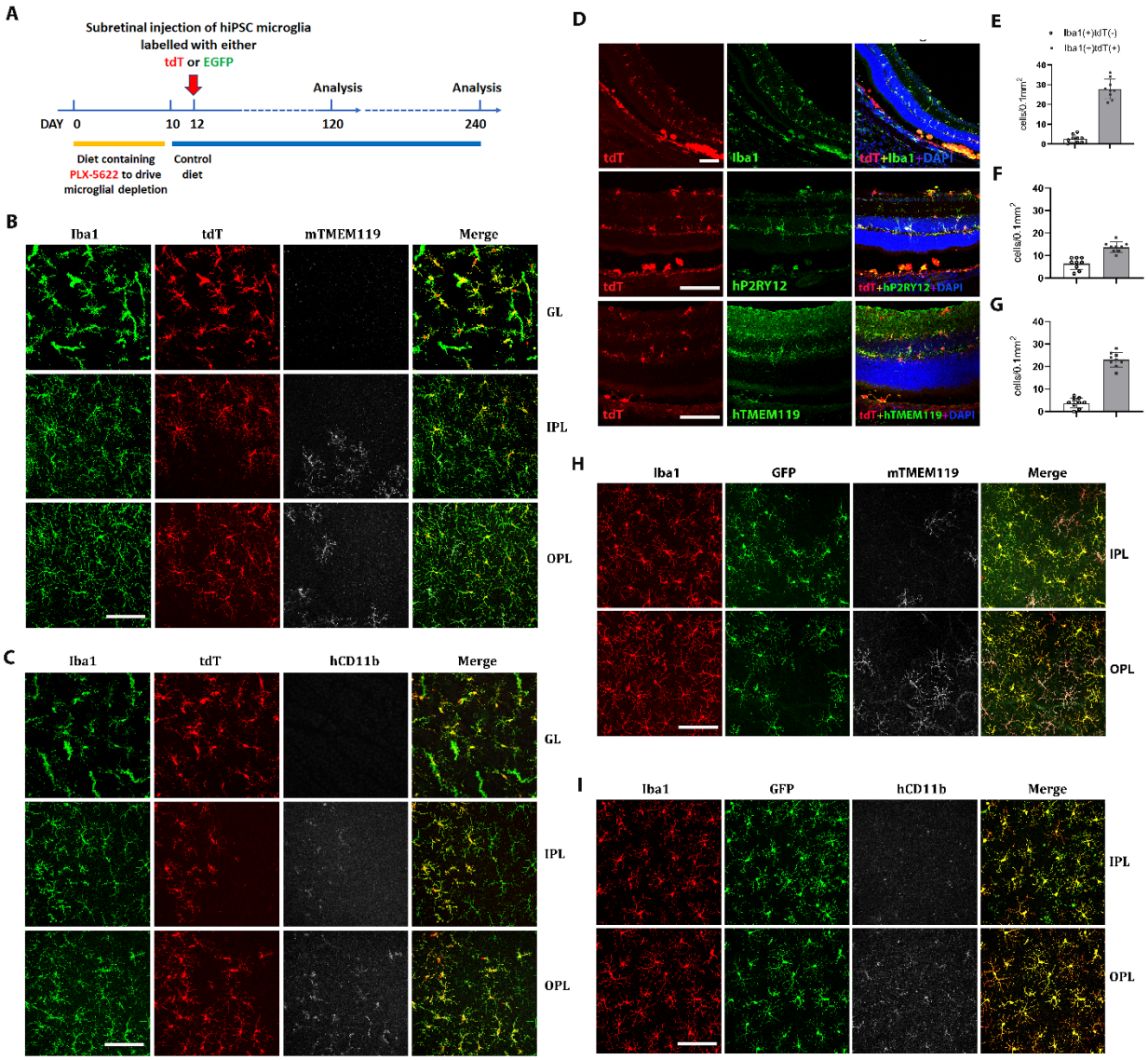

Figure 5. Human iPSC-derived microglia cells integrated into mouse retina and formed stable homeostasis after subretinal injection for 4 months. (A) The schematic diagram shows the timeline of

the experiments. The Plx5622 diet was administrated to 2-month-old Reg2-/-;IL2rg-/-;hCSF1+/+ mice for ten days, then switched with a normal chow; at day 12, the human iPSC-derived microglia cells which were labeled with tdTomato or EGFP were xenotransplanted into mouse subretinal space. The samples were harvested four months after transplantation. (B) The retinal flat mount showed microglia cells in the ganglion cell layer (GL), inner plexiform layer (IPL), and outer plexiform layer (OPL) with Iba1 (green) and mouse TMEM119 (Far-red) staining. The human microglia cells showed tdTomato positive. Scale bar = 100µm. (C) The retinal flat mount showed human CD11b staining only in tdTomato+ human microglia cells. Scale bar = 100µm. (D) The retinal section showed human iPSC-derived microglia cells integrated into whole retinal layers (top panel) and positively stained with human P2ry12 and TMEM119 microglia signature markers. Scale bar = 100µm. The microglia cell number in GL, IPL, and OPL of host mouse retina were counted: mouse microglia cells (Iba1+, tdT-) and grafted human microglia cells (Iba1+,tdT+) were shown in (E), (F) and (G), respectively. (H) and (I) showed EGFP-labeled human iPSC-derived microglia cells in the IPL and OPL of the flat-mount retina with mouse TMEM119 staining (H) and human CD11b staining (I). These results demonstrated that the infiltration of grafted hiPSC-derived microglia cells into the mouse retina is general in nature and not cell-line specific. Scale bar = 100µm.

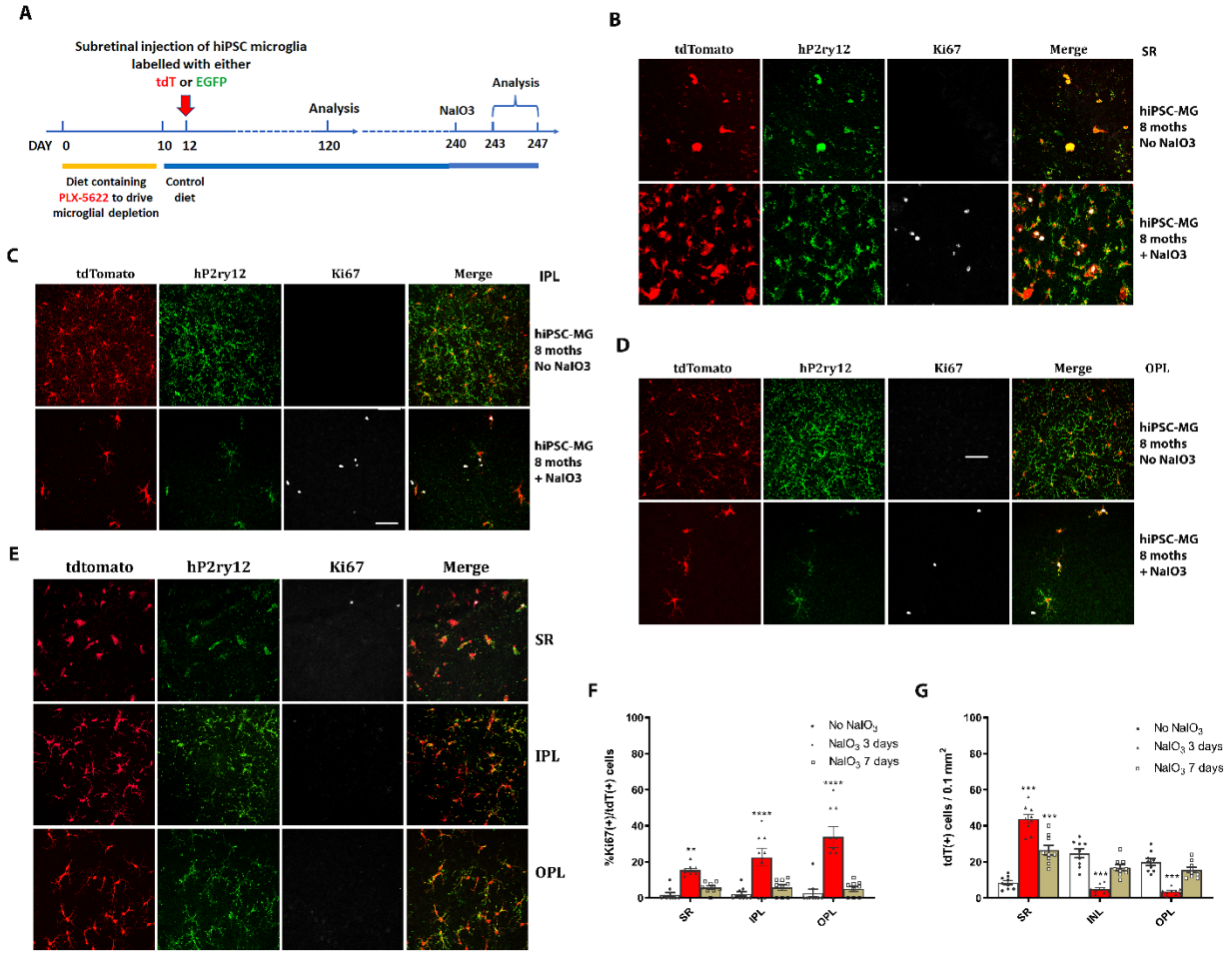

Figure 6. Migration and proliferation of homeostatic human iPSC-derived microglia cells in the mouse retina after RPE cells injury. (A) The schematic diagram shows the procedure of the experiment. After eight months of xenotransplantation, the NaIO3 (30mg/kg body weight) was injected into the mice through I.P. injection. The samples were harvested at 3 and 7 days after NaIO3 administration. (B) RPE-choroid flat-mount showed the microglia cells in the subretinal space. The tdtomato+ human microglia cells were stained with human P2ry12(green); the dividing cells were labeled with Ki67(Far red). The results indicated that tdtomato+ human microglia cells were attracted to the subretinal space in NaIO3-treated mice retina compared to non-NaIO3 injection (G). Some tdtomato+ & P2ry12+ human microglia cells started dividing as shown Ki67+ (F). Scale bar = 60µm. (C) and (D) showed the number of P2ry12+&tdtomato+ human microglia cells in IPL (C) and OPL (D) decreased; some of them showed Ki67+ staining, Scale bar = 60µm. The cell count results showed in (F) and (G). (E) The retinal flat mount showed the number of P2ry12+&tdtomato+ human microglia cells in IPL and OPL that were repopulated, and the cells stopped dividing with lost the Ki67 staining at seven days after NaIO3 injection. The cell numbers were shown in (F) and (G). Scale bar = 60µm.

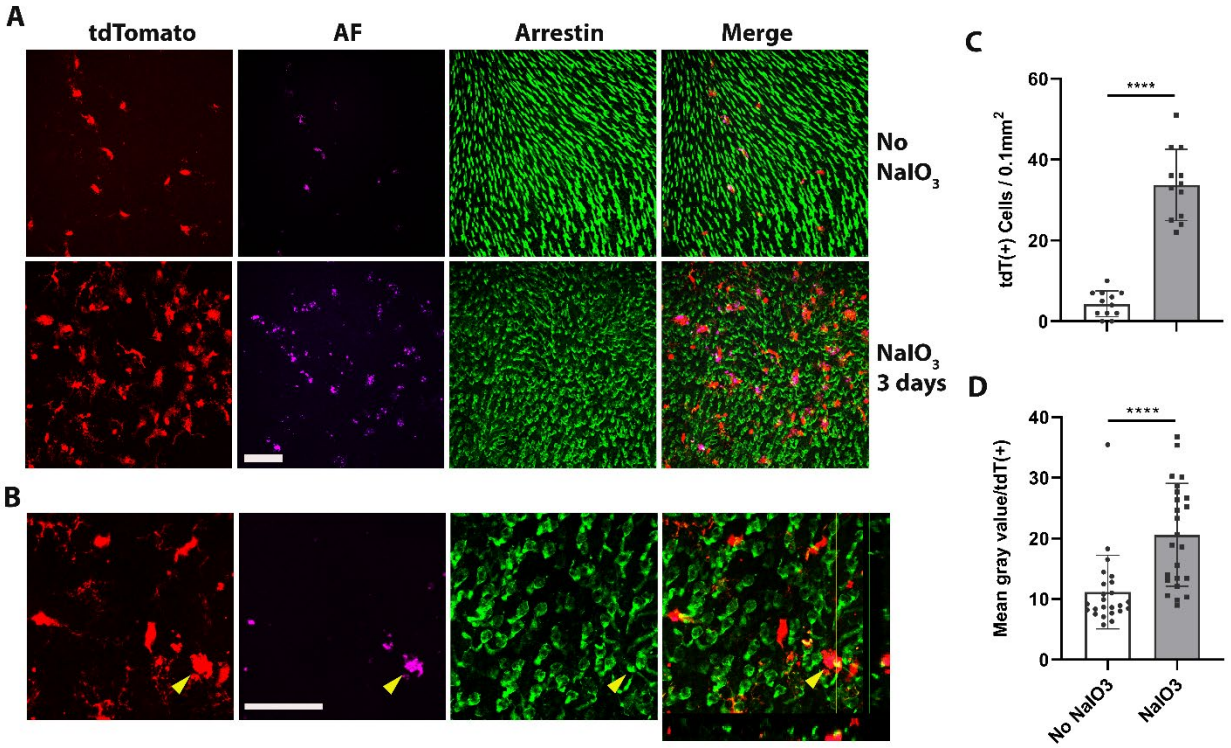

Figure 7. Dyshomeostasis human iPSC-derived microglia cells in the mouse retina phagocytose dead photoreceptor cells/debris after RPE cell injury. (A) Dyshomeostasis human microglia cells (tdtomato+) accumulated in the photoreceptor cell layer after 3 days of NaIO3-induced RPE cell injury compared with no NaIO3 administration. The photoreceptor cells stained with cone arrestin (green), autofluorescent showed in magenta. Scale bar = 60µm. (B) High magnificent and side view image showed human microglial cells (red) co-labeled with photoreceptor cells arrestin staining (green) after 3 days of NaIO3 injury. The yellow triangle showed the colocalized tdT+ human microglia cell and arrestin+ cone photoreceptor cell. Scale bar =40µm. (C) The number of human microglial cells in the photoreceptor layer; (D) The mean gray value of autofluorescent in each human microglia cell. **** P<0.0001.